the plant journal

SEB SOCIETY FOR EXPERIMENTAL BIOLOGY

*The Plant Journal* (2024) doi: 10.1111/tpj.16649

# Arabidopsis SNARE SYP132 impacts on PIP2;1 trafficking and function in salinity stress

**Guillermo Baena[1,#], Lingfeng Xia[1,#], Sakharam Waghmare[1,#], ZhiYi Yu[1], Yue Guo[2], Michael R. Blatt[1], Ben Zhang[2] and Rucha Karnik[1,*]**

[1]*Plant Science Group, School of Molecular Biosciences, College of Medical, Veterinary and Life Sciences, University of Glasgow, Bower Building, University Avenue, Glasgow G12 8QQ, UK, and*

[2]*School of Life Science, Shanxi University, Taiyuan, Shanxi 030006, China*

Received 6 September 2023; accepted 16 January 2024.

*For correspondence (e-mail rucha.karnik@glasgow.ac.uk).

[#]These authors contributed equally to the manuscript.

## SUMMARY

**In plants so-called plasma membrane intrinsic proteins (PIPs) are major water channels governing plant water status. Membrane trafficking contributes to functional regulation of major PIPs and is crucial for abiotic stress resilience. Arabidopsis PIP2;1 is rapidly internalised from the plasma membrane in response to high salinity to regulate osmotic water transport, but knowledge of the underlying mechanisms is fragmentary. Here we show that PIP2;1 occurs in complex with SYNTAXIN OF PLANTS 132 (SYP132) together with the plasma membrane $H^+$-ATPase AHA1 as evidenced through *in vivo* and *in vitro* analysis. SYP132 is a multifaceted vesicle trafficking protein, known to interact with AHA1 and promote endocytosis to impact growth and pathogen defence. Tracking native proteins in immunoblot analysis, we found that salinity stress enhances SYP132 interactions with PIP2;1 and PIP2;2 isoforms to promote redistribution of the water channels away from the plasma membrane. Concurrently, AHA1 binding within the SYP132-complex was significantly reduced under salinity stress and increased the density of AHA1 proteins at the plasma membrane in leaf tissue. Manipulating SYP132 function in *Arabidopsis thaliana* enhanced resilience to salinity stress and analysis in heterologous systems suggested that the SNARE influences PIP2;1 osmotic water permeability. We propose therefore that SYP132 coordinates AHA1 and PIP2;1 abundance at the plasma membrane and influences leaf hydraulics to regulate plant responses to abiotic stress signals.**

**Keywords: membrane traffic, SNARE, aquaporin, stomata, transport, *Arabidopsis thaliana*.**

## INTRODUCTION

Global climate change is predicted to significantly alter the frequency and magnitude of droughts on Earth, affecting cultivated land and causing fresh-water scarcity (FAO, 2019). Drought contributes to increased soil salinity and inflicts osmotic stress on land plants affecting plant growth, development and fitness (Ariga et al., 2017; Flowers, 2004; Liu, Liu, et al., 2022; Wehner et al., 2017). Elevated soil salinity is a major challenge for crop production in arid regions worldwide. Salinity stress induces phytohormone signalling and drives molecular changes in plant cells involving signal recognition and transduction leading to downstream effects on gene regulation (Basu et al., 2016; Gupta et al., 2020; Zhang, Zhu, et al., 2022). The effects of salt stress on the plant are similar to that of drought stress and include rapid changes to cell expansion rates in shoots and inhibition of stomatal opening (Munns & Tester, 2008).

Vesicle traffic in plant cells plays a crucial role in cellular morphogenesis and the regulation of membrane transport for plant responses to environmental stress (Bassham & Blatt, 2008; Kwon et al., 2020). The close coordination between the membrane transport and trafficking pathways underpins plant growth and stomatal responses (Grefen et al., 2011; Karnik et al., 2017; Klejchova et al., 2021; Wang et al., 2018). Constitutive vesicle traffic delivers newly synthesised proteins and facilitates membrane turnover (Grefen et al., 2011; Jürgens, 2004). At the plasma membrane cargo-specific exocytosis, endocytosis and cycling of transporters and ion channels control their abundance and partake in functional regulation of osmotic solute transport (Eisenach et al., 2012; Grefen et al., 2011; Karnik et al., 2017; Sutter et al., 2007; Xia et al., 2019). The trafficking of membrane-enclosed vesicles to and from the plasma membrane accommodates reversible changes in plant cell volume, and these mechanisms are at the centre

of dynamic control of the stomatal pore (Meckel et al., 2007).

As in all eukaryotes, Soluble N-ethylmaleimide-sensitive-factor attachment protein receptors, so-called SNAREs, contribute to vesicle traffic and are localised to target and vesicle membranes where they bind in complex to drive vesicle fusion in plants (Bassham & Blatt, 2008; Karnik et al., 2017; Pratelli et al., 2004). SNAREs are classified on the basis of the highly conserved amino acid (Q [Gln] or R [Arg]) residues at the centre of the SNARE domain (Bock et al., 2001; Fasshauer et al., 1998; Lin & Scheller, 2000). In *Arabidopsis thaliana*, Qa-SNAREs SYNTAXIN OF PLANTS 121 (SYP121 = SYR1/PEN1) and SYNTAXIN OF PLANTS 122 (SYP122) drive the bulk of secretory traffic at the plasma membrane together with an evolutionarily ancient SNARE SYNTAXIN OF PLANTS 132 (SYP132); these proteins bind with R-SNAREs VESICLE-ASSOCIATED MEMBRANE PROTEIN 721 (VAMP721) and VESICLE-ASSOCIATED MEMBRANE PROTEIN 722 (VAMP722) and with the Qbc-SNARE SOLUBLE N-ETHYLMALEIMIDE-SENSITIVE FACTOR ADAPTOR PROTEIN 33 (SNAP33) (El Kasmi et al., 2013; Enami et al., 2009; Ichikawa et al., 2014). The three homologous Qa-SNAREs contribute to environmental stress response mechanisms in the plant (Kwon et al., 2020). They share over 60% sequence similarity and have overlapping functions, but they also have distinct roles (Rehman et al., 2008; Waghmare et al., 2018). For example, SYP121 is essential for abiotic stress tolerance, affecting programmed closure in stomata and growth through regulation of the $K^+$ channels (Eisenach et al., 2012; Grefen et al., 2015; Honsbein et al., 2009). SYP132 drives defence-related secretory traffic to inhibit bacterial pathogens. Unusually, it also mediates hormone-regulated endocytic traffic of plasma membrane proton ATPases (PM $H^+$-ATPases), influencing plant growth and immunity (Baena et al., 2022; Kalde et al., 2007; Xia et al., 2019).

Plasma membrane $H^+$-ATPases energise the transport of osmotic ions and water flux across plant cell membranes generating turgor for plastic cell expansion and 'acid growth' (Falhof et al., 2016; Hager, 2003; Hager et al., 1980; Hager & Moser, 1985; Klejchova et al., 2021; Michelet & Boutry, 1995; Palmgren & Morsomme, 2019; Sze et al., 1999). Plasma membrane $H^+$-ATPase function is sensitive to hormonal cues and tracks plant responses to both biotic and abiotic signals (Baena et al., 2022; Kaundal et al., 2017; Yamauchi et al., 2016). Abiotic stress signals, including those which involve the water stress hormone abscisic acid (ABA), down-regulate plasma membrane $H^+$-ATPase function to promote stomatal closure and reduce water loss to protect the plant against dehydration (Jezek et al., 2021; Klejchova et al., 2021). Post-translational modifications modulate plasma membrane $H^+$-ATPase activity at the plasma membrane (Fuglsang & Palmgren, 2021; Hager, 2003; Haruta et al., 2015). In parallel, SNARE-assisted membrane trafficking underpins plasma membrane $H^+$-ATPase functional regulation and impacts plant growth, stomatal function and pathogenesis (Baena et al., 2022; Fuglsang & Palmgren, 2021; Hager et al., 1991; Xia et al., 2019, 2020; Xue et al., 2018).

Water flux across the cell and vacuolar membranes facilitates osmoregulation and maintains turgor in plant cells (Maurel & Chrispeels, 2001) essential for cell expansion, growth and stomatal function (Ding & Chaumont, 2020; Jezek & Blatt, 2017; Meckel et al., 2007). Aquaporins, the so-called plasma membrane intrinsic proteins (PIPs), are water channels that account for a majority of water flux affecting turgor and osmoregulation in plant cells (Chaumont & Tyerman, 2014). PIPs are small transmembrane proteins (21–34 kDa) that are subdivided into two homology subgroups, PIP1 and PIP2, each with multiple isoforms in Arabidopsis (Alexandersson et al., 2005; Postaire et al., 2010). Four PIP isoforms (PIP2;1, PIP2;2, PIP2;6 and PIP2;7) account for much of the hydraulic conductivity in the Arabidopsis rosette and three (PIP2;1, PIP2;2 and PIP2;4) affect guard cell water flux (Blatt et al., 2014; Ding & Chaumont, 2020; Grondin et al., 2015) and water permeation under abiotic stress (Grondin et al., 2015). Additionally, aquaporins are implicated in disease and pathogen immunity in both animals (Yang, 2017) and plants (Zhang et al., 2019). A stringent control of both PIP density and conductance regulates water transport across the plasma membrane in plant cells (Alexandersson et al., 2005; Chaumont & Tyerman, 2014; Hachez et al., 2013, 2014; Luu & Maurel, 2013). Together, the plasma membrane $H^+$-ATPase and PIP activities consolidate water and ion transport across the plasma membrane for physiological, developmental and adaptive responses of plants to biotic and abiotic challenges (Baena et al., 2022; Chaumont & Tyerman, 2014; Ding & Chaumont, 2020; Klejchova et al., 2021; Liu et al., 2009; Rodrigues et al., 2017; Vilakazi et al., 2017; Wang et al., 2018). How is PIP traffic regulated under abiotic stress and how is this traffic coordinated with plasma membrane $H^+$-ATPase activity? The answer to these questions will clearly be central to addressing challenges centred around the integration of multifactorial stress responses in plants.

We show here that both PIP and plasma membrane $H^+$-ATPase proteins occur within trafficking SNARE SYP132 complexes. These interactions were identified initially using mass spectrometry of SNARE-co-immunoprecipitant complexes obtained from purified Arabidopsis leaf tissue and confirmed using yeast-based protein–protein interaction assays. These, and additional experimental data indicate that the plasma membrane $H^+$-ATPase AHA1, and the aquaporins PIP2;1 and PIP2;2 associate within a SYP132-complex that is sensitive to abiotic stress. Compromising SYP132 functionality altered PIP2;1 distribution at the

plasma membrane and suppressed the impacts of salinity and osmotic stress in transgenic Arabidopsis. We propose that AHA1 and PIP2;1 association within the SYP132-complex at the plasma membrane coordinates their trafficking and regulates water and proton transport for plant responses to abiotic stress.

## RESULTS

### Aquaporins and the plasma membrane $H^+$-ATPase AHA1 co-immunoprecipitate in complex with the SNARE SYP132

Initial co-immunoprecipitation experiments with GFP-SYP132 (Figure 1a) identified PIP2 isoforms as major components in complex with the SNARE. Co-immunoprecipitant proteins were obtained from Arabidopsis stably expressing the green fluorescent protein (GFP)-tagged SNARE driven by its native promoter (Ichikawa et al., 2014; Xia et al., 2020). As experimental control and to discount non-specific interactions, we used transgenic Arabidopsis (pCaMV 35S: GPI-GFP) expressing GFP-fused glycosyl-phosphatidylinositol (GPI) membrane anchor peptide (Zhang et al., 2018). Purified membrane fractions from leaf tissue were applied on GFP-trap resin (Chromotek). After washing, the GFP-SYP132 co-immunoprecipitant proteins that bound to the resin were eluted (Figure S1a) and identified by mass spectrometry (MS) analysis. Proteins bound specifically with SYP132 were determined by discounting those proteins which co-immunoprecipitated with GPI-GFP (Table S1). A broad categorisation of the SYP132 interactors was carried out based on molecular functions, associated biological processes and cellular components by Gene Ontology annotation (http://pantherdb.org/) (Figure 1b). This analysis showed that among the 59 unique proteins recovered (Figure 1b), most were membrane-localised proteins contributing to water and proton transport as well as in biotic and abiotic stress responses. Notably, the SNARE interacted with plasma membrane $H^+$-ATPase, aquaporin PIPs and the proteins involved in clathrin-mediated endocytosis, CLATHRIN HEAVY CHAIN 1 (CHC1), CLATHRIN HEAVY CHAIN2 (CHC2) and CLATHRIN LIGHT CHAIN 2 (CLC2) (Figure 1b; Table S1).

In Arabidopsis, the plasma membrane water channels PIP2;1 and PIP2;4 share high sequence similarity and contribute to the bulk of water transport (Blatt et al., 2014; Grondin et al., 2015). Therefore, we verified SYP132 binding with these major PIP isoforms using a mating-based yeast GPI-signal peptide-anchored split ubiquitin (GPS) system. Previous application of the yeast GPS system (Zhang et al., 2018) with SYP132 showed a strong interaction with the $H^+$-ATPase AHA1 (Xia et al., 2019). For the binding assay, $SYP132^{\Delta C}$ fused CubPLV bait protein is localised to the plasma membrane by the GPI-anchor peptide Exg2. Protein binding is reported through a rescue of yeast growth even when bait protein expression is suppressed using 500 μM methionine. The expression of the bait and prey proteins in yeast cells was verified using immunoblot (Figure S1b,c). Binding with AHA1 was tested in parallel and served as positive control, the results indicating a differential interaction with PIP1;2, PIP2;1 and PIP2;4 (Figure 1c). These data identify the PIPs as new interacting partners of the plasma membrane trafficking SNARE SYP132.

### SYP132 association with AHA1, PIP2;1 and PIP2;2 is affected in salinity and osmotic stress

Transcript levels of PIP1;2, PIP2;1 and PIP2;4 are highly abundant in the leaf tissue, and these isoforms constitute majority of the water channel proteins in most of the plant, especially in the leaf tissue including guard cells (Alexandersson et al., 2005; Groszmann et al., 2023). Therefore, we tracked SYP132 interactions in Arabidopsis leaves using co-immunoprecipitation (Co-IP) assays. We observed that both AHA1 and PIP2 (PIP2;1 and PIP2;2) presence within the SYP132 complex was differentially altered under abiotic stress. Antibodies that specifically bind Arabidopsis AHA1, PIP1 (PIP1;1, PIP1;2, PIP1;3, PIP1;4 and PIP1;5) and PIP2 (PIP2;1 and PIP2;2) were used to detect the native proteins (Figure 2a,b). We purified plasma membranes from Arabidopsis leaf tissue using two-phase partitioning (Baena et al., 2022). As described above, input plasma membrane suspension was applied in excess of the binding capacity of the resin and following washes, GFP-SYP132 co-immunoprecipitant proteins were eluted for analysis. To examine the impact of abiotic stress on SYP132 binding, sets of 4-week-old *SYP132p*:GFP-SYP132 Arabidopsis plants were treated for 2 h prior to membrane fractionation with water (control), 200 mM sodium chloride (NaCl) solution to evoke salinity stress, or 75 mM mannitol to impose osmotic stress. Mannitol is a growth-repressive compound that mimics drought stress and is commonly used to trigger abiotic stress responses in plants (Verslues et al., 2006). Eluted GFP-SYP132 co-immunoprecipitant complexes were resolved using SDS-PAGE and analysed by immunoblot (Figure 2a). Immunoblot band intensities were measured using densitometry to calculate binding relative to the GFP-SYP132 bait (Figure 2c–e). These data showed that GFP-SYP132 interacts with AHA1, PIP1 and PIP2 proteins under control conditions in purified plasma membrane fractions. Although SYP132 binding with AHA1 is known to be enhanced during bacterial pathogenesis (Baena et al., 2022), we found that AHA1 binding in the SYP132 co-immunoprecipitant complex was significantly reduced under sodium chloride and mannitol stress (Figure 2c). Relative to the control, sodium chloride or mannitol treatments showed no significant effects on PIP1 (PIP1;1, PIP1;2, PIP1;3, PIP1;4 and PIP1;5) in complex (Figure 2d). However GFP-SYP132 association with PIP2

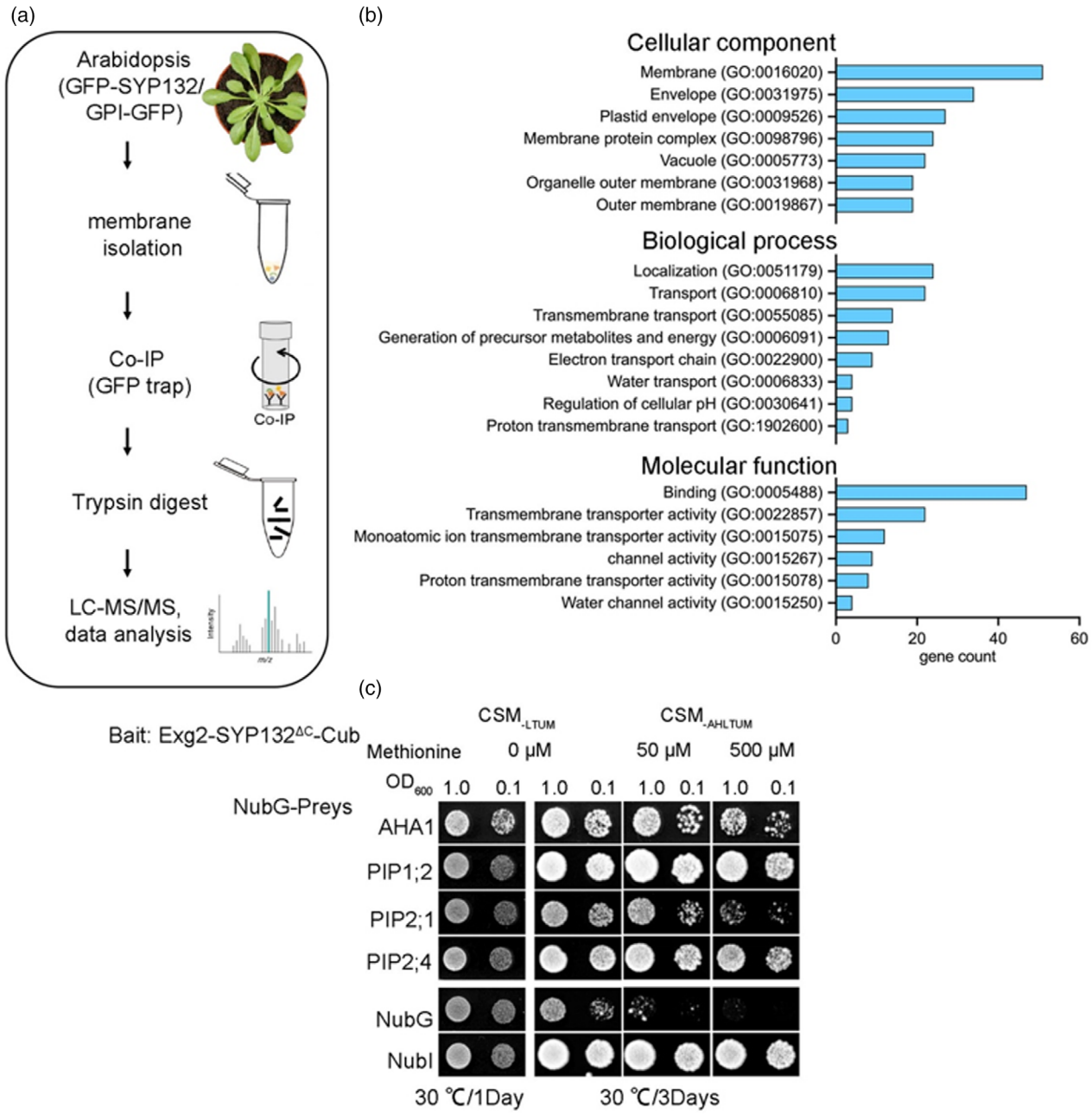


**Figure 1.** SNARE SYP132 co-immunoprecipitant complexes at the plasma membrane include $H^+$-ATPase and PIP proteins (also see Figure S1).
(a) Mass spectrometry analysis workflow. GFP-SYP132 or GPI-GFP co-immunoprecipitant proteins that were bound, washed and eluted using GFP-trap columns (verified using SDS-PAGE; see Figure S1a). Samples were trypsin digested and analysed using mass spectrometry (LC–MS/MS). The MS data was analysed (see Methods) to identify proteins bound within the SYP132 co-immunoprecipitant complex.
(b) Bar graph depicts Gene Ontology (GO) annotation (http://pantherdb.org/) categories of SYP132 co-immunoprecipitants identified in the MS analysis (see Table S1) based on cellular component, biological processes and molecular functions.
(c) Yeast mating-based split-ubiquitin (SUS) with GPI Signal Peptide-Anchored Split-Ubiquitin (GPS) system to test the interaction between bait $SYP132^{\Delta C}$ ($SYP132^{Methionine\ 1\text{-}Glutamate\ 270}$) and prey proteins AHA1, PIP1;2, PIP2;1 and PIP2;4. Bait proteins were fused with the Exg2-GPI signal peptide for membrane anchoring and at the N-terminus, and CubPLV at the C-terminus. The prey proteins were fused with N-terminal NubG. Experimental controls include bait expression with NubG (negative) and NubI (positive). Diploid yeasts were dropped at OD600 1.0 and 0.1 dilution and yeast growth was observed on CSM medium ($CSM_{-LTUM}$) without leucine (Leu, L), tryptophan (Trp, T), uracil (Ura, U) and Methionine (Met, M) to verify mating and on CSM medium ($CSM_{-AHLTUM}$) without adenine (Ade, A), histidine (His, H), Leu, Trp, Ura and Met to identify bait-prey interactions. Additional Met in the $CSM_{-AHLTUM}$ suppresses bait expression therefore yeast in these mediums indicates strong interactions with the prey. Incubation was carried out for 1 day on $CSM_{-LTUM}$ and 3 days on $CSM_{-AHLTUM}$ media. Bait and prey protein expression in the yeast cells was verified using immunoblot analysis (see Figure S1b,c). Also see Figure S4.

(PIP2;1 and PIP2;2) proteins increased significantly by over two-fold (Figure 2e). Immunoblots for endoplasmic reticulum-resident lumen-binding protein BiP and plasma membrane SNARE SYP121 verified the high purity (>99%) of the plasma membrane fractions (Figure S2). Taken together these data suggest that SNARE SYP132 co-immunoprecipitant complexes at the plasma membrane include PIP2 (PIP2;1 and PIP2;2) and AHA1, and that these complexes may be altered under abiotic stress.

### SYP132 influences the PIP2 abundance at the plasma membrane

In Arabidopsis, the hormone ABA induces plasma membrane $H^+$-ATPase interactions with a subset of trafficking SNARE proteins to suppress the abundance of the transporters at the plasma membrane (Baena et al., 2022; Xue et al., 2018). Endocytic traffic of the AHA1 in response to ABA, auxin and bacterial pathogens is mediated by SYP132 (Baena et al., 2022; Xia et al., 2019, 2020). SNAREs are also thought to play an important role in PIP traffic and influence plant hydraulics: (Hachez et al., 2014) showed that the Qa-SNARE SYP121 and the Qc-SNARE SYP61 mediate PIP2;7 traffic to the plasma membrane and influence water transport. Therefore, we asked if PIP endocytosis from the plasma membrane was SYP132-dependent.

Wild-type Arabidopsis plants were treated for 2 h in 200 mM sodium chloride (NaCl) solution or in 75 mM mannitol to induce abiotic stress as above. As a control, plants were also treated with water prior to the isolation of microsomal membranes. Purified plasma membrane and internal membranes were obtained using two-phase partitioning and the fractions were resolved on SDS-PAGE for immunoblot analysis (Figure 3a). We tracked native AHA1 to determine effects on $H^+$-ATPase traffic and distribution under the abiotic stress conditions. Previous studies showed that over-expression of SYP132 deters or suppresses its functions; SNARE availability and secretion of antimicrobials at the plasma membrane is reduced and AHA1 redistribution from the plasma membrane is altered in these situations (Baena et al., 2022, Xia et al., 2019, 2020). Hence, to evaluate the influence of the SNARE on PIP protein trafficking under abiotic stress, Arabidopsis transgenics over-expressing the SNARE protein [35S:RFP-SYP132, SYP132-OX (Baena et al., 2022)], referred to from here on as $SYP132^{DT}$ (SYP132-Deterrent), were challenged in parallel with wild-type plants in these experiments.

We found a five-fold decrease in native PIP2 protein density at the plasma membrane in plants treated with NaCl and mannitol as compared to control conditions and a corresponding increase in the density of PIP2 in internal membrane fractions (Figure 3a,d). By contrast, the abundance of AHA1 proteins at the plasma membrane increased by over two-fold in response to NaCl and mannitol challenge (Figure 3a,e). Nevertheless, the densities of PIP1, SYP132 and SYP121 at the plasma membrane were not affected in the wild-type and $SYP132^{DT}$ plants when compared to the control. Complementary analysis using qRT-PCR showed no significant changes in the levels of *SYP132*, *PIP1;4* and *PIP2;1* transcripts following NaCl and mannitol treatments relative to control (Figure S3a–c). Corresponding to these data, no significant changes were observed in levels of PIP1, PIP2 and SYP132 proteins in total microsomal fractions following NaCl and mannitol treatments in both wild-type and $SYP132^{DT}$ Arabidopsis relative to the control (Figure 3b–d; Figure S3d). As expected, there was a significant decrease in AHA1 density at the plasma membrane in $SYP132^{DT}$ plants when compared to the wild-type plants in control conditions (Figure S3e). A corresponding decrease in PIP2 density at the plasma membrane was observed, but PIP1 protein levels remained unchanged (Figure 3a; Figure S3f,g). These data show that PIP2 protein abundance at the plasma membrane is regulated in response to NaCl and mannitol treatments as is the case for AHA1. The SNARE SYP132 influences both AHA1, PIP2;1 and PIP2;2 traffic from the plasma membrane, likely promoting the redistribution of the channels from the plasma membrane under NaCl and mannitol stress.

### SYP132 downregulates PIP2;1 water permeability and influences abiotic stress tolerance

While the experiments above indicated a role for SYP132 in PIP traffic, they do not rule out additional actions through changes in the specific activity of the aquaporins at the membrane. Thus, we asked if SYP132 affects water transport activity directly following heterologous expression in *Xenopus laevis* oocytes. For this purpose, we used swelling assays as described before (Canessa Fortuna et al., 2019). As expected, expression of Arabidopsis PIP2;1 in oocytes enhanced osmotic water permeability and promoted swelling as compared to oocytes expressing SYP132 alone as a control. However, in oocytes co-expressing PIP2;1 and the SNARE, oocyte swelling was reduced as levels of SYP132 increased (Figure 4a–c). There is no evidence in the literature to indicate that plant SNAREs are functional in vesicle trafficking in oocytes. Therefore, together with data showing suppression of PIP2;1 density in $SYP132^{DT}$ plants (Figure 3; Figure S3g), we suggest that SYP132 impacts both PIP2;1 density and function at the plasma membrane.

Rosette hydraulics and environmental regulation are dictated by PIP2;1 activity (Prado et al., 2013). To determine if SNARE SYP132 regulation of the aquaporin proteins affects the hydraulic status of the plants, we measured leaf relative water content in Arabidopsis wild-type and $SYP132^{DT}$ plants treated with water, NaCl or mannitol as before. Plants were grown for 5 weeks under standard 150 $\mu mol\ m^{-2}\ sec^{-1}$ light in 8 h light/16 h dark cycles at

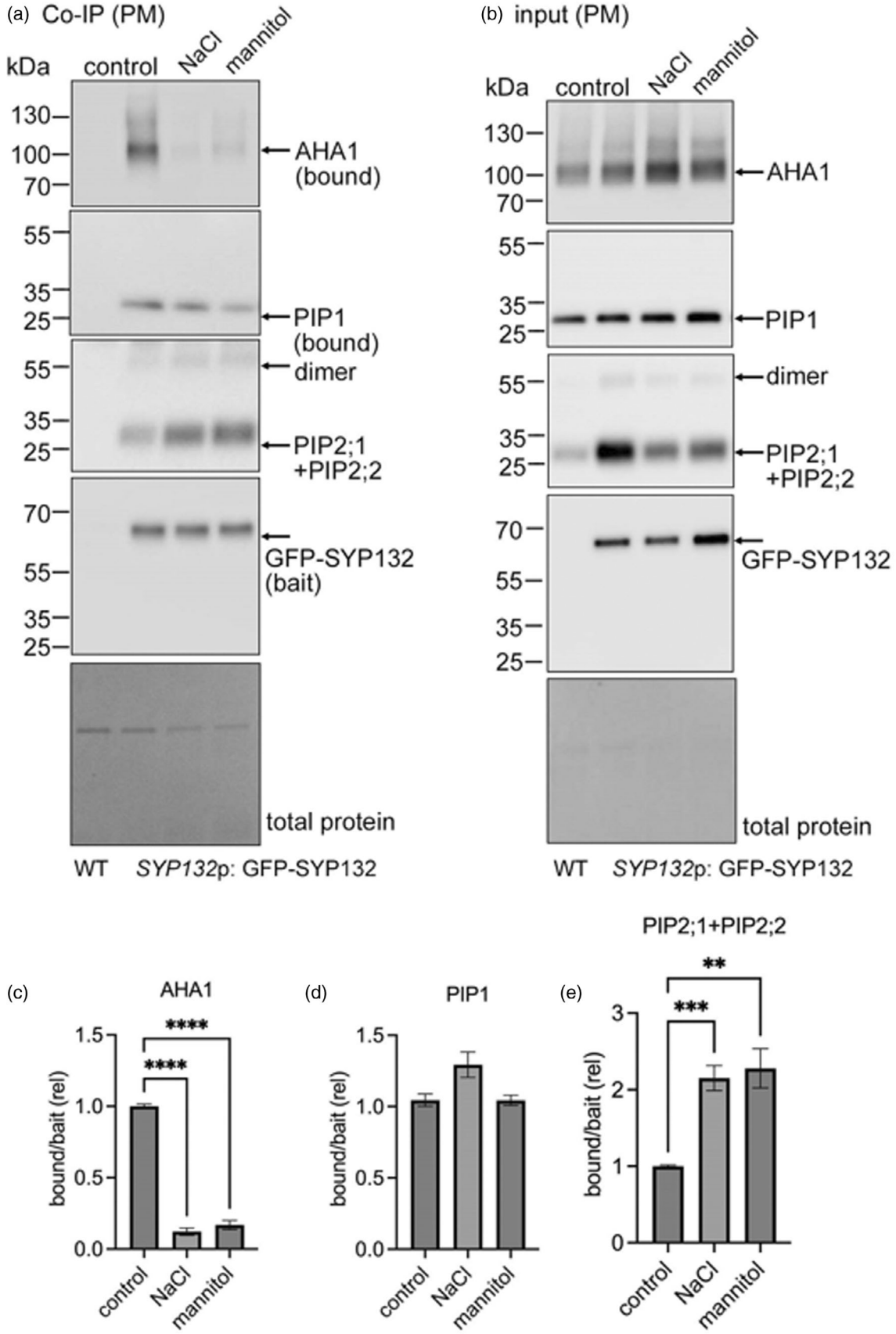

**Figure 2.** SNARE SYP132 binding with AHA1 and PIPs in plasma membrane fractions is altered in salinity and mannitol stress (see also Figure S2).
Immunoblots (representative) showing co-immunoprecipitation (Co-IP) assays (a) and plasma membrane (PM) fractions used as input (b) for the Co-IP. Five-week-old *SYP132*p: GFP-SYP132 Arabidopsis plants were treated with water (control), 200 mM NaCl or 75 mM mannitol for 2 h prior to isolation of microsomal membranes. Purified plasma membrane suspensions were applied to GFP-trap resin and co-immunoprecipitant protein complexes were eluted following washes to remove loosely bound proteins. Plasma membranes from wild-type plants that lack GFP proteins were used as experimental controls to verify that any proteins non-specifically bound to the resin were washed out. Immunoblots (a,b) show bound AHA1 (approx. 100 kDa) detected using anti-AHA1 antibodies (first panels), PIP1 proteins (approx. 28 kDa) detected using antibodies that bind PIP1;1, PIP1;2, PIP1;3, PIP1;4 and PIP1;5 (second panels), PIP2 proteins (approx. 28 kDa monomer, 56 kDa dimer) detected using antibodies that bind both PIP2;1 and PIP2;2 isoforms in Arabidopsis (third panels) and GFP-SYP132 (bait, approx. 63 kDa) detected using anti-GFP antibodies (fourth panel). Band intensities were measured using densitometry analysis using ImageJ software and normalised to total protein (Coomassie) in each lane (bottom panels). Endoplasmic reticulum resident BiP proteins (approximately 74 kDa) were detected using anti-BiP antibody and were absent in the plasma membrane input samples, indicating purity of fractions (also see Figure S2).
(c–e) Mean ± SE relative densities of AHA1 (c), PIP1 proteins (d) and PIP2 (PIP2;1 and PIP2;2) (e) bound relative to GFP-SYP132 bait in the Co-IP assay. Graphs for PIP2 (PIP2;1 and PIP2;2) represent a sum of intensities of monomer and dimer bands detected in each lane. Statistically significant differences were determined using Brown-Forsythe and Welch ANOVA with Dunnett's T3 multiple comparisons test, represented by * = $P < 0.03$, ** = $P < 0.002$, *** = $P < 0.0002$ and **** = $P < 0.0001$. In the experiments ≥3 plants were used for each treatment, $N = 3$.

22°C/18°C (see 'Methods' section) prior to harvesting. We found that leaf relative water content (RWC) for SYP132$^{DT}$ plants was significantly higher compared to wild-type plants under all conditions and the plants were more resilient to abiotic stress (Figure 4d,e). Thus, SYP132 appears to influence the plant water status and abiotic stress tolerance.

How might the SNARE coordinate the association with both aquaporins and plasma membrane $H^+$-ATPases? One clue comes from additional yeast Tri-SUS analysis (Zhang et al., 2021) which showed that PIP2;1 and $H^+$-ATPase AHA1 are likely to occur in a complex with the SNARE SYP132 (Figure S4). The Tri-SUS system detects tripartite bait and prey interactions involving a third methionine-repressible partner protein (Figure S4a). Yeast growth is observed if the bait and prey interaction is bridged by a third partner protein. In this assay co-expression of the SNARE as a partner facilitated the assembly of PIP2;1-SYP132-AHA1 complex. We found that there was no yeast growth if AHA1 was expressed as a partner protein (Figure S4b). It is expected that direct interactions between the two transporters are unlikely. Therefore, data suggest that the SNARE might be important for bringing together the water channels and plasma membrane $H^+$-ATPase proteins in the membrane to coordinate water and proton transport in plants, either through synergistic or competitive binding processes. We discuss this point further below.

## DISCUSSION

In nature, plants are generally challenged with diverse and interacting stresses that are most likely to occur simultaneously or in sequence (Pandey et al., 2015). Drought stress is often associated with salinity and osmotic challenges influence plant growth, immunity, productivity and water use causing enormous losses in agricultural production (Zhang et al., 2020). Conversely, plant-microbe interactions are reported to affect abiotic stress tolerance (Gigli-Bisceglia & Testerink, 2021; Ma et al., 2020; Saijo & Loo, 2020). Central to these processes is membrane transport powered by the plasma membrane $H^+$-ATPases and the hydraulic control of turgor and cell expansion (Blatt et al., 2014; Chaumont & Tyerman, 2014; Maurel & Chrispeels, 2001). Energisation by the plasma membrane $H^+$-ATPases affects a repertoire of environmental stress and endogenous hormonal signals (Bellati et al., 2016; Chaumont & Tyerman, 2014; Maurel et al., 2015, 2016; Rodrigues et al., 2017; Sadura et al., 2020).

Multiple environmental and endogenous factors that influence water homeostasis in plant cells rely on post-translational regulation of transporters which includes tetramer assembly, phosphorylation, protein–protein interactions and endocytic recycling (Bellati et al., 2016; Hachez et al., 2014; Luu & Maurel, 2013; Maurel et al., 2015; Verdoucq et al., 2014; Wudick et al., 2015). The current understanding is that membrane trafficking dictates PIP abundance at the plasma membrane and contributes to the regulation of water transport in response to stress (Besserer et al., 2012; Hachez et al., 2014; Verdoucq et al., 2014; Wudick et al., 2015). Some SNARE proteins that mediate in vesicle traffic can also interact with aquaporins directly to influence water transport (Barozzi et al., 2018; Besserer et al., 2012; Hachez et al., 2014). Although much remains unknown, these relatively new concepts potentially redefine the knowledge of mechanisms controlling plant hydraulics.

We uncover here a new role for the plasma membrane trafficking SNARE SYP132 in coordinating proton and water transport in plant cells. Thus, in Arabidopsis we find (1) that SYP132 regulates the abundance of the aquaporin PIP2;1 and its closest homologue PIP2;2 together with $H^+$-ATPase AHA1 at the plasma membrane; (2) that PIP2;1 and PIP2;2 associate within SYP132-complexes that include AHA1 and are altered under salinity and drought conditions and finally (3) that the SNARE strongly affects PIP2;1 osmotic water permeability on heterologous expression and it impacts leaf relative water content and influences plant resilience to abiotic stress *in vivo*.

### SYP132-associated trafficking under abiotic stress

Membrane vesicle trafficking affects ion transport by controlling the population and availability of ion channels and

transporters at the plasma membrane and is thus important for cellular homeostasis, growth, immunity and responses to the environment (Blatt et al., 2014; Grefen et al., 2011; Honsbein et al., 2011; Klejchova et al., 2021; Rodriguez-Furlan et al., 2019; Wang et al., 2018). There is a significant body of work that describes the importance of membrane traffic in the regulation of $K^+$ channels (Karnik et al., 2017), and more recently, that of the plasma membrane $H^+$-ATPases (Baena et al., 2022; Xia et al., 2019, 2020; Xue et al., 2018).

Similarly, there is a growing body of evidence that trafficking affects aquaporin density and is important for

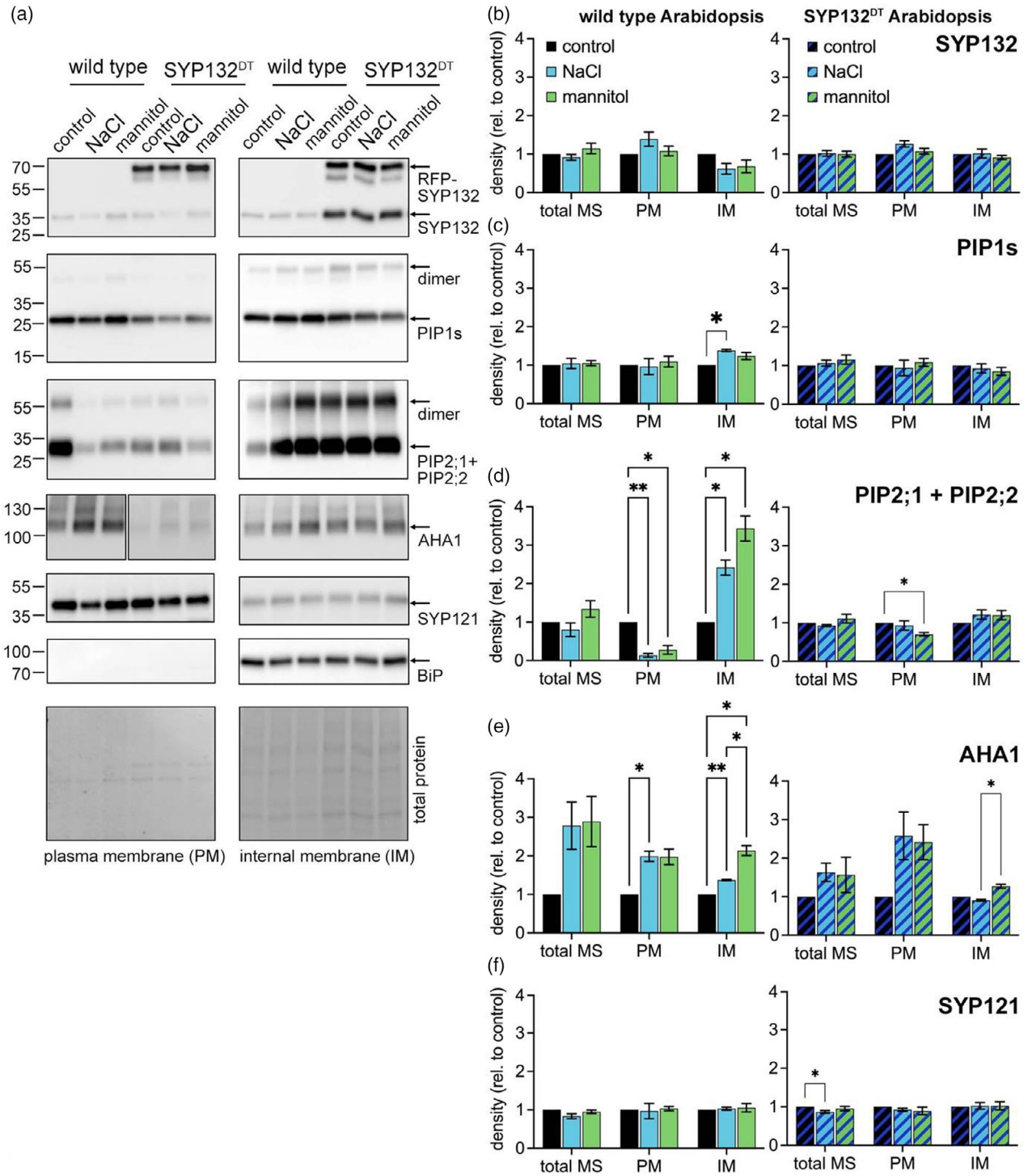

**Figure 3.** SNARE SYP132 influences the PIP and AHA1 density and redistribution at the plasma membrane in abiotic stress (see also Figure S3).
(a) Immunoblot analysis of plasma membrane and internal membrane fractions from 4- to 5-week-old wild-type or SYP132-dominant negative (SYP132$^{DT}$, 35S:RFP-SYP132) Arabidopsis leaves resolved using SDS-PAGE. Immunoblot analysis of microsomal membranes is in Fig S3d–g. Plants were treated with water (control), 200 mM sodium chloride (NaCl) or with 75 mM mannitol solutions in water for 2 h prior to membrane fractionation. Immunoblots (representative) show plasma membrane (PM, left panels) and internal membrane (IM, right panels) respectively. Native SYP132 is detected at approx. 35 kDa and RFP-SYP132 bands at 61 kDa (first panels) using anti-SYP132 antibodies; PIP1 proteins (approx. 28 kDa monomer, 56 kDa dimer) are detected using antibodies that bind PIP1;1, PIP1;2, PIP1;3, PIP1;4 and PIP1;5 (second panels); PIP2 proteins (approximately 28 kDa monomer, 56 kDa dimer) are detected using antibodies that bind both PIP2;1 and PIP2;2 isoforms in Arabidopsis (third panels) and AHA1 (approximately 100 kDa) is detected using anti-AHA1 antibodies (fourth panels). To detect SNARE SYP121 (approximately 38 kDa), anti-SYP121 antibody was used (fifth panels). Lumen-binding protein BiP (approx. 74 kDa), a marker for internal membranes was detected using anti-BiP antibodies (sixth panels). Purity of the plasma membrane fractions was estimated at >99% using BiP bands as reference. Total protein was detected using Coomassie stained immunoblot membrane (bottom panels). Black lines (left) indicate positions of molecular mass markers, and black arrows (right) indicate expected band positions.
(b–f) Mean ± SE protein density relative to control. Plots include protein densities in total microsomal, plasma membrane and internal membrane fractions in wild-type Arabidopsis (left panels) and SYP132$^{DT}$ Arabidopsis (right panels) for SYP132 (b), PIP1s (c), PIP2 (PIP2;1 + PIP2;2) (d), AHA1 (e) and SYP121 (f). Values were obtained from densitometric analysis of immunoblots, normalised total protein detected using Coomassie stain, relative to water treated control. Statistically significant differences were determined using ANOVA using Tukey's multiple comparisons test, represented by * = $P < 0.03$ and ** = $P < 0.002$, $N = 3$ using ≥3 plants for every sample in each experiment.
About 10-fold more total protein was loaded for internal membrane fractions than for plasma membrane fractions, precluding a direct comparison between these blots. Figure S3 shows corresponding analysis for transcript levels (Figure S3a–c), immunoblots (representative) of total MS fractions (Figure S3d), and protein abundance relative to wild-type control (Figure S3e,f).

the regulation of water transport (Chaumont et al., 2005; Maurel et al., 2015; Paudel et al., 2017; Ueda et al., 2016; Wudick et al., 2015). SNAREs are implicated in aquaporin trafficking and influence cell membrane water permeability: for instance, Besserer et al. (2012) found that post-Golgi trafficking and water channel activity of maize PIP2;5 is regulated by SYP121, a plasma membrane Qa-SNARE which is also involved in vesicle traffic and regulation of voltage-gated $K^+$ channels (Karnik et al., 2017). In Arabidopsis, SYP121 and Qc-SNARE SYNTAXIN OF PLANTS 61 (SYP61) regulate proper delivery of PIP2;7 to the plasma membrane through direct interactions with the water channels (Hachez et al., 2014). SNARE binding has since been attributed to cytosolic domains on PIP2;7 (Laloux et al., 2020), suggesting that putative mechanisms might exist which help confer specificity to the regulation of aquaporin trafficking and function.

Previous analysis of Arabidopsis PIP2;1 suggested that internalisation of the aquaporin in response to salinity stress contributes to its down-regulation at the plasma membrane (Li et al., 2011). Our findings that PIP2;1 and PIP2;2 are internalised from the plasma membrane in a SYP132-dependent manner now add a key insight into the regulation of these aquaporins. In our hands, salinity and osmotic stress treatments drive PIP2;1 redistribution from the plasma membrane to internal membrane fractions and these responses are suppressed in SYP132$^{DT}$ transgenic Arabidopsis (Figure 3) with deterred SYP132 functions. Furthermore, the impacts of SYP132 appear specific for the PIP2 isoforms and do not extend to PIP1-type aquaporins (Figure 3).

It is worth noting that Li et al. (2011) employed chemical blockers to suggest that PIP2;1 endocytosis relies on two distinct pathways, one mediated by clathrin and the other dependent on the protein partitioning to lipid raft membrane microdomains (Li et al., 2011). Indeed, studies using clathrin mutant Arabidopsis have shown that the SNARE SYP132 mediates clathrin-sensitive endocytosis of AHA1 (Xia et al., 2019). We suggest therefore that SYP132 might be involved in the clathrin-dependent trafficking pathways of PIP2;1 and PIP2;2. A subset of RARE COLD INDUCIBLE 2 (RCI2) proteins is reported to bind and promote CsPIP2;1 endocytosis in *Camelina sativa* under salinity stress (Kim, Park et al., 2020). Overexpression of RCI2D affects lipid vesicle accumulation in *Camelina* roots (Kim, Lim et al., 2020; Kim et al., 2022), and it may be that RCI2 is involved in clathrin-independent trafficking pathways of the aquaporins. None of the Arabidopsis RCI2 isoforms were detected within the SYP132-complexes in our mass spectrometry experiments (Figure 1; Table S1). Hence, SYP132-mediated endocytic pathways, at least in Arabidopsis shoots, are likely to be distinct from lipid-raft pathways.

At the plasma membrane PIP2;1 and PIP2;2 density is significantly reduced in the SYP132$^{DT}$ relative to the wild-type Arabidopsis under control conditions (Figure S3). It may be that SYP132 cycling (Baena et al., 2022) enhances PIP2 endocytosis in these plant lines. Irrespective of the mechanism, however, shoot growth and relative water content measurements in the SYP132$^{DT}$ plants showed that manipulating SYP132 suppresses aquaporin abundance at the plasma membrane (Figure 4d,e). Thus, SYP132 underpins both PIP2 and AHA1 traffic at the plasma membrane influencing plant resilience to abiotic stress challenges.

As expected, in SYP132$^{DT}$ plants total SYP132 (SYP132 + RFP-SYP132) density at the plasma membrane is higher compared to wild-type plants (Figure 3). A decrease is observed in both AHA1 and PIP2s levels in the wild-type plants following NaCl and mannitol treatments (Figure 3). By contrast, in the SYP132$^{DT}$ plants, these abiotic stress conditions did not appreciably alter PIP2 density (Figure S3e–g). We note that the expression of RFP-SYP132 still showed a substantial reduction in AHA1 at the plasma

membrane, much as was shown previously (Xia et al., 2019). Therefore, the presence of RFP-SYP132 clearly has a profound impact itself on traffic. The fact that it also leads to a reduction in PIP2 density at the plasma membrane argues against any explanation that overexpressing the RFP-SYP132 protein suppresses native SYP132 function. To some extent these characteristics appear to mimic the iSNARE phenomenon. However, iSNAREs cause tonoplast accumulation and the inhibition of fusogenic properties of a SNARE protein (De Benedictis et al., 2013; Di

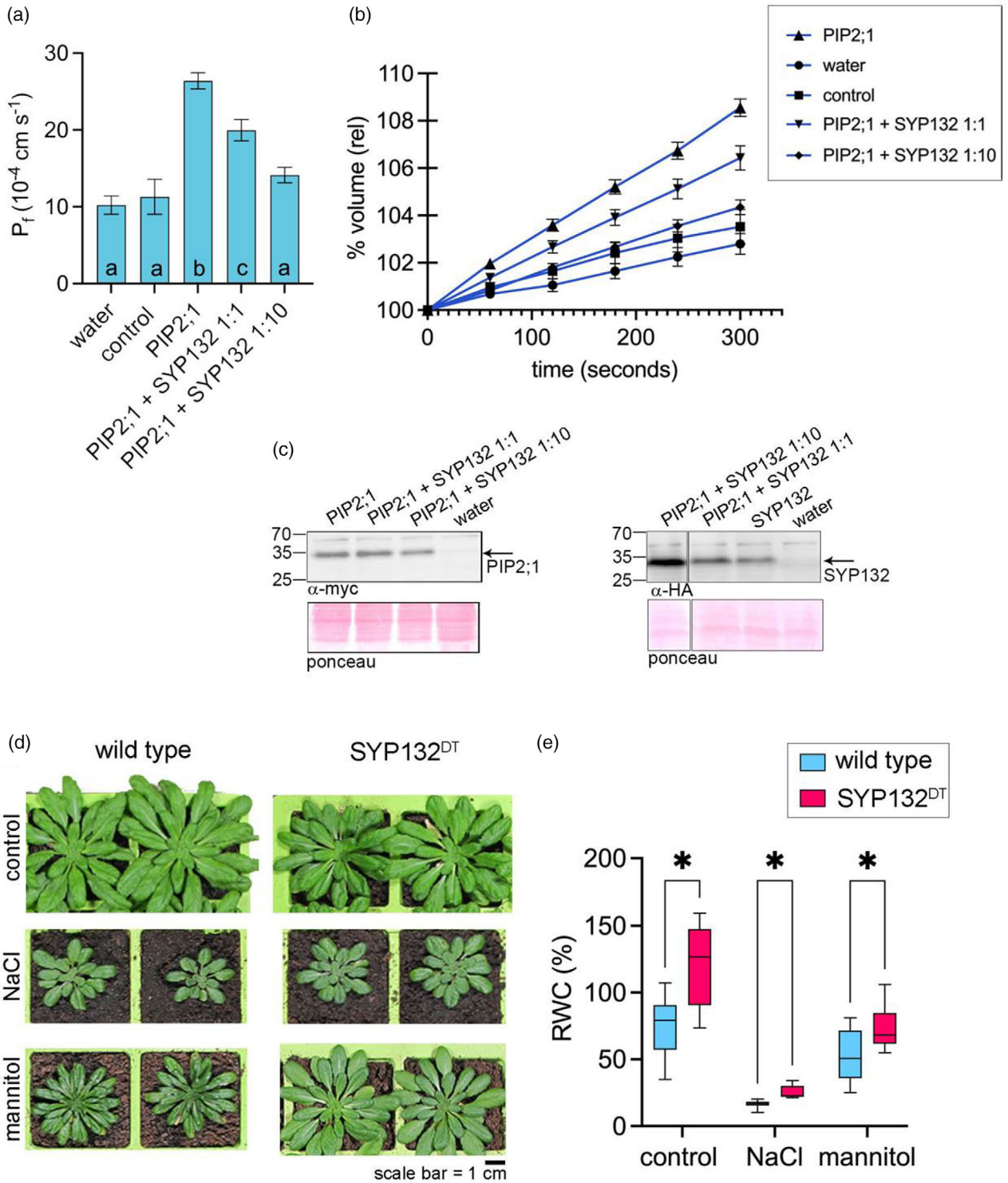

**Figure 4.** SYP132 regulates PIP2;1 osmotic water permeability and leaf relative water content.
(a) Osmotic water permeability coefficient (Pf) measured from *Xenopus oocytes* injected with cRNA for heterologous expression of Arabidopsis SYP132 and PIP2;1 proteins. Plots are mean $P_f \pm$ SE from oocytes expressing SYP132 (control) or PIP2;1 and co-expressing PIP2;1 and SYP132, using cRNA ratios 1:1 and 1:10. The non-injected oocytes (water) served as negative control. Data are representative of three independent experiments. Statistical significance using ANOVA is represented using letters ($P < 0.001$), $n = 13$–23 oocytes.
(b) Time course of the relative volume change in oocytes from (A). The oocytes were imaged before injection (0 sec) and after injection with corresponding cRNA at 60, 120, 180, 240 and 300 sec. Data are means ± SE, $n = 13$–23 oocytes.
(c) Immunoblots detecting the expression of proteins in oocyte water transport assays (A and B). Following analysis, oocyte lysates in Laemmli buffer were resolved on SDS-PAGE to detect the expression PIP2;1 and SYP132 using anti-cMyc and anti-HA antibodies, respectively (panels on left). Immunoblots show bands for proteins: PIP2;1 (approx. 33 kDa) and SYP132 (approx. 38 kDa); and black lines (left) indicate positions of molecular mass markers, and black arrows (right) indicate expected band positions. Total proteins in each lane of the immunoblot membrane were detected using ponceau stain (panels on right).
(d) Photographs (representative) of wild-type or SYP132-dominant negative Arabidopsis ($SYP132^{DT}$, 35S: RFP-SYP132) rosettes. Plants were grown under standard 150 μmol $m^{-2}$ $sec^{-1}$ light in 8 h light/16 h dark cycles at 22°C/18°C and treated with water (control), 200 mM NaCl or 75 mM mannitol to induce stress for 4–5 weeks. Scale bar = 1 cm.
(e) Relative Water Content (RWC %) in wild-type or $SYP132^{DT}$ Arabidopsis rosettes in control (water), NaCl or mannitol stress conditions; c.f (d). Data are mean ± SE. * represent statistical significance determined in pairwise comparisons using Mann–Whitney tests, ($P < 0.05$), $n = 3$, using 5 or more plants each.

Sansebastiano, 2013). We did not observe any appreciable increase in the accumulation of RFP-SYP132 within internal membrane fractions following NaCl or mannitol treatments in wild-type or $SYP132^{DT}$ Arabidopsis (Figure 3a,b).

We know from previous work that when SYP132 expression is upregulated, the SNARE undergoes rapid endocytic cycling which suppresses its density and deters its functions at the plasma membrane (Baena et al., 2022). Moreover, Xia et al. (2019) demonstrate that overexpression of the so-called SYP132-Sp3 dominant negative peptides instead promotes plasma membrane $H^+$-ATPase distribution at the plasma membrane. The new data thus upholds previous hypothesis that SYP132 abundance is stringently regulated in plant cells. We highlight that in the absence of viable null mutants, the $SYP132^{DT}$Arabidopsis obstructs the functions of this SNARE and serves as a research tool.

### SYP132-mediated traffic and AHA1 density at the plasma membrane under stress

Plasma membrane $H^+$-ATPase function is stringently regulated through post-translational modifications and membrane trafficking (Falhof et al., 2016; Fuglsang & Palmgren, 2021; Palmgren & Morsomme, 2019; Sondergaard et al., 2004). Past studies show that during bacterial pathogenesis, AHA1 binding with SYP132 is enhanced and these interactions affect AHA1 endocytosis. Conversely, the plasma membrane $H^+$-ATPase regulates SNARE cycling from the plasma membrane, influencing defence-related secretory traffic and pathogen immunity (Baena et al., 2022). We have now found that in response to salinity and osmotic stress, SYP132 binding with AHA1 is significantly reduced at the plasma membrane (Figure 2a–c). These observations correspond with an increased abundance of the transporters in purified plasma membrane fractions (Figure 3a,b,e). Clearly, binding with the SNARE is a pre-requisite for AHA1 endocytosis, as is noted for ABA-induced internalisation of the plasma membrane $H^+$-ATPases (Xia et al., 2019).

How do these data reconcile AHA1 activity in abiotic stress? In response to salt stress, sodium efflux into the apoplast and its compartmentalization inside the vacuole is energised by plasma membrane $H^+$-ATPases (Falhof et al., 2016; Munns et al., 2006). Thereby, salt stress induces plasma membrane $H^+$-ATPase activation through phosphorylation and 14–3-3 protein binding (Janicka-Russak et al., 2013). Since AHA1 activation is thought to occlude SYP132 binding (Xia et al., 2019), the new findings support the hypothesis that AHA1 regulation in salt stress conditions is linked to its activation.

### SYP132-complexes of AHA1 and PIP2 aquaporins impact on transport

Interactions between PIP1 and PIP2 isoforms are widely reported over the past two decades (Jozefkowicz et al., 2016; Shibasaka et al., 2021; Zelazny et al., 2007) and are thought to be the part of a conserved mechanism driving PIP1 proteins to the plasma membrane in heterotetrameric conformations (Bienert et al., 2018). Even so, each isoform is thought to independently facilitate water flux and may have separate regulatory mechanisms. Here we establish that SYP132 interacts with PIP2;1 as well as other water channel isoforms including PIP2;4 and PIP1;2: native protein complexes in plasma membrane fractions of Arabidopsis leaf tissue were detected using immunoblot (Figure 2). We also identified binary protein–protein interactions using yeast-based mbSUS assays (Figure 1c). This approach has in the past demonstrated SYP132 binding with $H^+$-ATPase AHA1 (Baena et al., 2022; Xia et al., 2019), SNARE interactions with PIPs (Hachez et al., 2014) and the binding between SYP121 and $K^+$ ion channels (Grefen et al., 2015; Honsbein et al., 2011).

We propose that SYP132 coordinates the PIP2 and plasma membrane $H^+$-ATPase abundance and functions during salinity stress. In support, we have found that PIP2;1 and the plasma membrane $H^+$-ATPase AHA1 proteins associate within SYP132 complexes at the plasma membrane (Figures 1 and 2). A previous mass

spectrometry analysis examining PIP1;2 and PIP2;1 interactomes in root tissue detected AHA1 (Bellati et al., 2016). Selective PIP2;1 binding with the SNARE SYP132 was also detected in these screens following NaCl treatment of root tissue (Bellati et al., 2016). SNARE–Aquaporin interactions were not the primary focus of these studies, nevertheless proteomics data support a role for syntaxins and clathrin in aquaporin regulation and point to additional protein partners affecting PIP trafficking (Bellati et al., 2016). We uncover here that in Arabidopsis shoots, SYP132-complexes include AHA1, aquaporin PIP2;1 and its homologues as well as several proteins of the clathrin machinery (Figures 1 and 2). In our experiments, salinity and mannitol challenges enhanced PIP2;1 association within the SNARE-complex while AHA1 binding was significantly reduced (Figure 2) while PIP1 density at the plasma membrane and binding within SYP132-complexes remained unchanged. Additionally, yeast Tri-SUS assays that probe tripartite protein binding suggested that SYP132 may act as a conduit bringing together PIP2;1 and AHA1 complexes (Figure S4). These are exciting findings: they suggest that assembly of PIP2;1-SYP132-AHA1 complexes at the plasma membrane could be a mechanism for coordinating proton and water transport in the shoots. Previous studies indicate that AHA1 binding with SYP132 is localised to the N-terminal Habc domain on the SNARE and that deletion of this domain inhibits AHA1 traffic from the plasma membrane (Baena et al., 2022). Further studies to isolate specific binding motifs/domains may advance the understanding of PIP2;1 interaction within the SNARE complexes and their timing with the binding to the $H^+$-ATPase.

Remarkably we have found that co-expression of PIP2;1 and SYP132 suppressed osmotic water uptake and associated swelling of *Xenopus laevis* oocytes (Figure 4a–c). Heterologous expression of PIP2;1 facilitates water permeability in *Xenopus* oocytes and the swelling response is attributed to aquaporin activity on the oocyte membrane (Grondin et al., 2015). We observed that increased SYP132 expression further reduced water uptake in these experiments, suggesting SYP132 dose-dependent effects (Figure 4a–c). It may be that increased SYP132 expression affects PIP2;1 traffic at the oocyte plasma membrane which suppresses water uptake. There is no evidence that plant SNAREs are functional in oocytes, despite over two decades of plant SNARE research, whereas trafficking of the PIPs is clearly mediated by native Xenopus SNAREs. Furthermore, we did not observe any obvious reduction in the PIP2;1 protein in the oocytes that may be attributed to endocytic degradation (Figure 4c). Although we cannot rule out that SYP132-mediated trafficking in the heterologous system, the observed effects are most easily explained if interactions with SYP132 alter PIP2;1 osmotic permeability in the oocytes.

**PIP2;1 and AHA1 in environmental response**

Finally, we note that the coordination of aquaporin and plasma membrane $H^+$-ATPase activities has immediate relevance to stomata and their regulation to balance $CO_2$ uptake for photosynthesis against water loss from the photosynthetic tissues (Jezek & Blatt, 2017; Lawson & Blatt, 2014; Melotto et al., 2017; Vialet-Chabrand et al., 2017; Wang et al., 2018). Stomatal regulation relies on the transport of osmotic solutes at the plasma membrane and the tonoplast as well as hydroactive water fluxes that control turgor and cell volume (Blatt et al., 2002; Grefen et al., 2011; Jezek et al., 2019, 2021; Jezek & Blatt, 2017; Lawson & Blatt, 2014; Vavasseur & Raghavendra, 2005; Zonia & Munnik, 2007). Stomata respond to a variety of environmental and endogenous factors including the water-stress hormone abscisic acid (ABA), light and pathogens (Jezek et al., 2019, 2021; Jezek & Blatt, 2017; Lawson & Blatt, 2014; Liu, Hou, et al., 2022; Melotto et al., 2017; Vavasseur & Raghavendra, 2005).

Relevant to this study, plasma membrane $H^+$-ATPase endocytosis contributes to the downregulation of plasma membrane $H^+$-ATPase activity at the plasma membrane (Fuglsang & Palmgren, 2021; Xia et al., 2019). In stomatal guard cells, these pathways promote closure of the stomatal pore to resist water loss in ABA (water-stress hormone) or in drought stress (Xue et al., 2018) and to promote stomatal defence against bacterial pathogens (Baena et al., 2022). Aquaporins impact disease and pathogen immunity in both animals (Yang, 2017) and plants (Zhang et al., 2019; Zhang, Shi, et al., 2022) and are deemed critical for stomata-pathogen interactions, a pattern conserved across plant species (Rodrigues et al., 2017; Zhang et al., 2019). Our analysis shows that SYP132 regulation of PIP2;1 has coordinate and opposing effects on AHA1 binding with the SNARE (Figures 1 and 2). High salt (NaCl) and mannitol give rise to an osmotic imbalance that is adjusted by stomatal closure and suppression of water transport activity to prevent water loss (Granot & Kelly, 2019; Jezek & Blatt, 2017). Both PIP2;1 and PIP2;2 have high water channel activity (Verdoucq et al., 2008) and are implicated in stomatal regulation in response to various environmental stress conditions and endogenous signals (Basu et al., 2016; Chaumont & Tyerman, 2014; Grondin et al., 2015; Hetherington & Woodward, 2003; Huang et al., 2020; Israel et al., 2021; Rodrigues et al., 2017; Zhang et al., 2019). Here we find that SYP132 influences PIP2;1 density and functions at the plasma membrane (Figures 3 and 4). We anticipate that SYP132 control of PIP2 trafficking, and activity affects the water status of the plant and is likely a key factor contributing to stomatal function.

In summary (Figure 5), we uncover a new role for the plasma membrane trafficking SNARE SYP132 in the regulation of PIP2;1 density and function in response to salinity

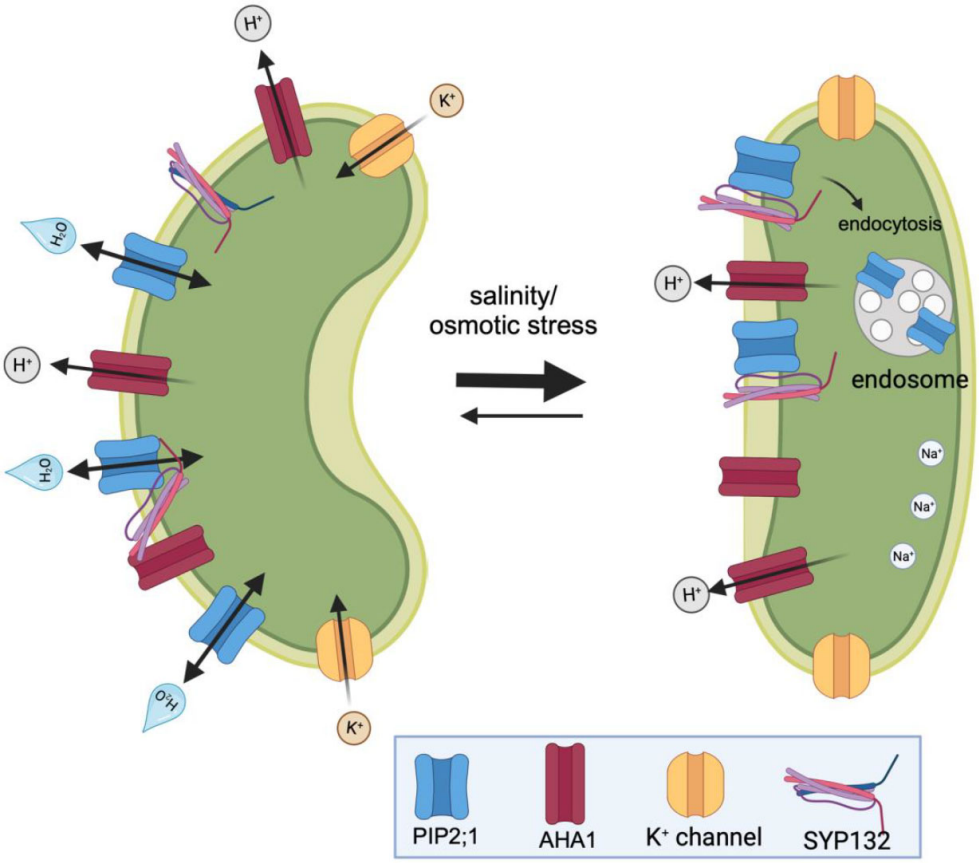


**Figure 5.** SYP132-mediated regulation of PIP2;1 and AHA1 during salinity stress. Schematic representation of our hypothesis for SYP132-mediated regulation of PIP2;1 and AHA1 in response to salinity and osmotic stress. A simplified model of stomatal guard cells is shown and represents reversible changes in cell volume that cause stomata to open (left panel) or close (right panel). Plasma membrane $H^+$-ATPases energise ion and water transport for turgor and increase in cell volume for stomatal opening. Secondary transporters, voltage-activated $K^+$ channels that drive osmotic solute uptake are shown; other transporters are not included in the schematic for simplicity. The trafficking SNARE SYP132 interacts with both PIP2;1 and AHA1 proteins at the plasma membrane. Salinity and osmotic stress cause a decrease in AHA1 binding with the SNARE, while PIP2;1 binding with SYP132 is increased and promotes PIP2;1 redistribution from the plasma membrane to endosomal membranes. AHA1 density is elevated and may facilitate proton transport to maintain ion homeostasis in elevated sodium ($Na^+$). In parallel, SYP132 binding with PIP2;1 suppresses the function of the water channels. In summary, SYP132 coordinates PIP2;1 and AHA1 density and functions at the plasma membrane during abiotic stress, thus contributing to stomatal closure to prevent dehydration. Schematic was created with BioRender.com.

and osmotic stress. Differential interactions of SYP132 with the PIP2;1 are enhanced following salinity challenge and PIP2;1 distribution at the plasma membrane is enhanced. Remarkably, these pathways appear to intersect with the coordinate regulation of AHA1 that is governed by the SNARE during pathogenesis. We find here that AHA1 binding with SYP132 is reduced and there is an increase in AHA1 density at the plasma membrane in response to NaCl. Thus, SYP132 is at the centre of an antiparallel association of PIP2 and of the $H^+$-ATPase that is affected by salinity.

## EXPERIMENTAL PROCEDURES

### Plant material, growth conditions and physiology experiments

Plants of *Arabidopsis thaliana* Columbia-0 ecotype (wild type) were used in the study. In addition, transgenic Arabidopsis stable lines used are described previously, namely the *35S CaMV*: RFP-SYP132, SYP132-OX (over expressor) Xia et al. (2019) which is referred to here as $SYP132^{Deterrent}$ = $SYP132^{DT}$, the *SYP132* native promoter-driven GFP-SYP132 (*SYP132p*:GFP-SYP132; Ichikawa et al., 2014), and *35S CaMV* promoter-driven GFP-fused with a hydrophobic signal sequence from a GPI protein (GFP-GPI; Zhang et al., 2018). *Arabidopsis thaliana* plants were grown on soil under standard conditions of 8 h light/16 h dark, 22°C/18°C cycle and 150 μmol $m^{-2}$ $sec^{-1}$ light and 60% restricted humidity for 4–5 weeks.

Plants were maintained under well-watered conditions with watering twice a week. Salt or osmotic stress was induced by bathing the plants in 200 mM NaCl or 75 mM mannitol respectively as described before (Karimi et al., 2021; Virk et al., 2015). For leaf RWC analysis (Sade et al., 2015), turgid and dry weights of 4-week-old Arabidopsis rosettes were measured. The RWC (%) was calculated as 100 × (fresh weight − dry weight)/(-turgid weight − dry weight). All the experiments were repeated three times using at least five plants for each line and treatment.

### Total RNA isolation and RT-qPCR analysis

Total RNA isolation and RT-qPCR analysis were described previously (Alexandersson et al., 2005; Xia et al., 2019). Briefly, total RNA was extracted using TRIzol Plus RNA Purification Kit (Invitrogen, Paisley, UK), and the isolated total RNA was quantified and used for cDNA synthesis. RT-qPCR reactions were performed using gene-specific primers (see Table S2) (Armengot et al., 2016; Jang et al., 2004). Fold change in the gene expression was calculated as $2^{-\Delta\Delta Ct}$ (Livak & Schmittgen, 2001) using reference gene, the mitochondrial 18S rRNA.

### Immunoblot analysis

Immunoblot assays were performed as described before, (Baena et al., 2022). Purified membrane fractions were solubilised in the Laemmli buffer, resolved on SDS-PAGE using 4%–20% gradient gels (Bio-Rad) and transferred to nitrocellulose membranes (Bio-Rad) using Transblot (Bio-Rad Laboratories, Watford, UK). Immunoblot membranes were incubated with 5% (w/v) non-fat dry milk in 1xTris-buffered saline (TBS; 150 mM NaCl, 50 mM Tris–HCl, pH 7.5, 0.1% [v/v] Tween-20) blocking solution prior to incubation with primary antibodies diluted in 2.5% (w/v) milk, 1xTBS. To detect native proteins expressed in Arabidopsis we used antibodies anti-SYP132 (1:3000; Baena et al., 2022), anti-AHA1 (1:3000; Baena et al., 2022), anti-PIP1 (1:5000; Agrisera AS09 487) recognising PIP1;1, PIP1;2, PIP1;3, PIP1;4, PIP1;5 isoforms, anti-PIP2 (1:5000; Agrisera AS09 491) that binds PIP2;1 + PIP2;2 proteins or anti-BiP (1:10000; Agrisera AS09 481) antibodies. GFP- and RFP-tagged proteins were detected using anti-GFP (1:5000; Chromotek 3 h9) and anti-RFP (1:5000; Chromotek 4f8) antibodies respectively. Membranes were washed using wash buffer (1×TBS), and membranes were incubated with secondary antibodies goat anti-rabbit- or goat anti-rat-horseradish peroxidase conjugate (1:20000; Agrisera AS09 602, AS10 1187). Proteins were visualised using SuperSignal West Pico PLUS Chemiluminescent Substrate (Thermo Fisher Scientific, Leicestershire, UK) and imaged by Fusion FX Chemiluminescence Imager (Vilber, France). Immunoblot band intensity was measured by densitometry using the ImageJ software and values were normalised against total protein in each lane detected using Coomassie or Ponceau stains.

### Co-immunoprecipitation assay

Protein homogenates from Arabidopsis leaf tissue were diluted with the binding buffer (PBS [10 mM Phosphate, 2.68 mM KCl, 140 mM NaCl, pH 7.45], 0.01% Triton X-100, 0.05 mM DTT, 0.01% CHAPS, protease inhibitor [Thermo Fisher Scientific]) and incubated with GFP-Trap® agarose beads (Chromotek, Proteintech Europe, UK) for 1 h at 4°C with gentle shaking. The beads were collected and washed three times with washing buffer (binding buffer with an additional 150 mM NaCl) and the bound proteins were eluted with 2× Elution buffer (50 mM Tris–HCl, pH 6.8, 5% w/v SDS, 2 mM EDTA, 0.1% Triton X-100, 50 mM DTT, 12% v/v glycerol, 0.05% w/v bromophenol blue).

### Mass spectrometry analysis

LC–MS/MS analysis was performed on a Dionex Ultimate 3000 RSLC nanoflow system (Dionex, Camberley, UK) and Orbitrap Elite mass spectrometer (Thermo Fisher Scientific). Each sample was digested using the Filter Aided Sample Preparations (FASP) method (Wisniewski et al., 2009) to generate tryptic peptides prior to mass spectrometry. Trypsin-digested peptides were loaded on a C18 trap column and then separated on a 50 cm Acclaim PepMap100 column (particle size 3 μm, internal diameter 75 μm) with linear gradient 5–35% buffer B (0.1% formic acid in 80% acetonitrile) over 135 min at a flow rate of 300 nl/min. Eluate from the column was introduced to the Orbitrap Elite MS by electrospray ionisation. The ionisation voltage was set to 1.7 kV and the ion transfer tube temperature to 220°C. The MS was operated in positive ion mode using collision-induced dissociation/higher energy collisional dissociation CID/HCD fragmentation methods for MS2. Full scan Fourier transform-based mass spectrometry (FTMS) spectra were acquired in the range from m/z 380.0 to 1800.0, with a resolution of 60 000. The maximum injection time for the FTMS full scan was set as 200 ms, reaching an automatic gain control (AGC) target value of $1 \times 10^6$. The three most intense peaks from each MS spectrum were selected for each fragmentation mode. Ions with the charge state 1+ were excluded from the fragmentation list. The HCD MS/MS scan was fixed to start from m/z 100.00 with a resolution of 15 000 using an MS2 AGC target of $5 \times 10^4$. The collision energy was set as 40% normalised collision energy (NCE). An isolation window of ±1.5 Da was applied to isolate precursor ions with dynamic exclusion of 20 sec. Every precursor ion was repeated twice within a duration time of 30 sec and was excluded for 20 sec. Ion trap mass spectrometry CID MS/MS scan spectra were acquired with 35% NCE and an AGC target of $1 \times 10^4$.

Acquired MS/MS spectra were analysed for protein identification using Proteome Discoverer 3.0 software (Thermo Scientific). Protein identification was performed using *in silico* spectral libraries generated with Proteome Discoverer 3.0 and Mascot search engine (v2.6.2, Matrix Science) against Arabidopsis taxonomy in NcbiAV (version 2017-1-30; 92 149 sequences), with a precursor mass tolerance of 10 ppm and fragment ion mass tolerance of 0.8 Da. Two missed cleavages for the trypsin digestion were permitted. Identified peptides were filtered with a cut-off criterion of a *q*-value of 0.01, corresponding to a 1% false-discovery rate (FDR) for highly confident peptide hits and a *q*-value of 0.05 (5% FDR) for peptide hits with moderate confidence. For protein identification, the criteria of a cut-off value of at least two unique high-confidence peptides per protein detected in at least two out of three replicates was used. Proteins detected in both GFP-SYP132 and GPI-GFP co-immunoprecipitant samples were considered as non-specific interactors for the SNARE and were excluded from further analysis. Ribosomal proteins detected in the assays were also excluded from the analysis since they do not regulate SNARE function.

Gene Ontology (GO) analysis of detected proteins describes biological process, molecular function or cellular component was carried out using the PANTHER Overrepresentation Test. All unique genes with biological process information for Arabidopsis (GO Ontology database DOI: 10.5281/zenodo.7942786 Released 2023-05-10) were used as the reference set (all genes in the database). *P*-values were calculated by the FISHER test and their false discovery rates (FDRs) were adjusted by the Benjamini–Hochberg method.

### In vitro cRNA synthesis and Xenopus oocyte swelling assay

For *Xenopus laevis* oocytes water transport assays, PIP2;1 was inserted into the pGT-cMyc-Dest vector, while SYP132 was cloned into the pGT-nHA-Dest vector (Zhang et al., 2015). The plasmids were then linearized, and capped RNA (cRNA) was synthesised in vitro using the mMESSAGE mMACHINE T7 High Yield Capped RNA Transcription Kit (Ambion, Invitrogen, Paisley, UK) as described by (Zhang et al., 2015). The quality of the RNA was

assessed using agarose gel electrophoresis, and the concentration was determined using a Nano-300 spectrophotometer (Hangzhou Allsheng Instruments, China).

Stage VI oocytes were obtained from mature *X. laevis* frogs, and the follicular cell layer was digested with 2 mg/ml collagenase (Sigma-Aldrich (Merck) Dorset, UK) for 20 min prior to injection with water (non-injected, negative control), or cRNA coding for PIP2;1 or SYP132. Injected oocytes were incubated at 18°C in ND96 solution (96 mM NaCl, 2 mM KCl, 1 mM $MgCl_2$, 1 mM $CaCl_2$ and 10 mM HEPES-NaOH, pH 7.4) supplemented with gentamycin (5 mg/L) for 3 days before recording. Changes in oocyte volume were monitored using an SZ680 zoom stereo microscope equipped with a colour camera (Chongqing Optec Instrument, China). Cell swelling in response to a four-fold dilution of ND96 buffer with distilled water was captured in still images, and the oocyte was treated as a growing sphere, allowing its volume to be inferred from its cross-sectional area using Image J software version 1.37 (NIH, USA). Oocyte osmotic water permeability coefficient (Pf) was determined by measuring the rate of osmotic oocyte swelling. Pf was calculated using the formula $Pf = V0[d(V/Vo)/dt]/[S\ Vw\ (Osm_{in}\text{-}Osm_{out})]$, where V0 represents the initial oocyte volume ($9 \times 10^{-4}$ $cm^3$), V/V0 denotes the relative volume, S is the oocyte surface area (0.045 $cm^2$), Vw represents the molecular volume of water (18 $cm^3$/mol), and $Osm_{in}\text{-}Osm_{out}$ represents the osmotic driving force (Canessa Fortuna et al., 2019; Fox et al., 2020). Osmolarities were measured using a vapour pressure osmometer (Vapro 5600, Wescor, USA).

## ACKNOWLEDGEMENTS

We thank Dr Christophe Maurel for sharing with us aquaporin antibodies. We acknowledge Dr Richard Burchmore and Glasgow Polyomics team for support with mass spectrometry, Amparo Ruiz-Prado for help with the logistics of plant propagation and George Boswell for supporting plant propagation work.

## AUTHOR CONTRIBUTIONS

RK conceptualised the work, GB, SW and RK planned experiments. GB carried out Co-IP and membrane fractionation assays and plant assays, LX and ZY carried out yeast SUS assays, and immunoblot analysis, SW did mass spectrometry experiments and data analysis, BZ and YG did Xenopus experiments. RK and MRB wrote the manuscript.

## FUNDING INFORMATION

This work was supported by grants from the Biotechnology and Biological Sciences Research Council (BB/S017348/1, BB/S506734/1, BB/X013383/1), Royal Society (RG160493), Royal Society University Research Fellowship (UF150364, URF\R\211002) to RK and Wellcome ISSF Excellence and Innovation Catalyst Funding (204820/Z/16/Z), BBSRC Agriculture, Health and Food funding (BB/W510658/1) to GB, and funding to BZ from the National Natural Science Foundation of China (Nos. 32000210 and 32272012), and Research Project Support by Shanxi Scholarship Council of China (No. 2021-015), and Funding Program for the Scientific Activities of Selected Returned Overseas Professionals in Shanxi Province (No. 20230003). China Scholarship Council PhD studentship funding supports LX (201706300012) and ZY (202006350012).

## CONFLICT OF INTEREST

The authors declare that the research was conducted in the absence of any commercial or financial relationships that could be construed as a potential conflict of interest.

## DATA AVAILABILITY STATEMENT

All relevant data can be found within the manuscript and its supporting materials. The mass spectrometry proteomics data have been deposited to the ProteomeXchange Consortium (http://proteomecentral.proteomexchange.org) via the PRIDE partner repository (Perez-Riverol et al., 2022) with the dataset identifier PXD048655.

## SUPPORTING INFORMATION

Additional Supporting Information may be found in the online version of this article.

**Table S1.** GFP-SYP132 co-immunoprecipitant proteins identified using mass spectrometry.

**Table S2.** RT-qPCR reactions were performed using gene-specific primers (Figure S3a–c).

**Figure S1.** Detection of proteins in mass spectrometry and yeast mbSUS assays.

**Figure S2.** Purified Plasma membrane (PM) fractions used in Co-IP assay.

**Figure S3.** Effect of NaCl and mannitol treatments on SYP132 and PIP transcripts and total protein levels.

**Figure S4.** SNARE SYP132 bridges AHA1 and PIP2;1 complexes in yeast Tri-SUS assays.

## REFERENCES

**Alexandersson, E., Fraysse, L., Sjövall-Larsen, S., Gustavsson, S., Fellert, M., Karlsson, M. *et al.*** (2005) Whole gene family expression and drought stress regulation of Aquaporins. *Plant Molecular Biology*, **59**, 469–484.

**Ariga, H., Katori, T., Tsuchimatsu, T., Hirase, T., Tajima, Y., Parker, J.E. *et al.*** (2017) NLR locus-mediated trade-off between abiotic and biotic stress adaptation in *Arabidopsis*. *Nature Plants*, **3**, 17072.

**Armengot, L., Caldarella, E., Marques-Bueno, M.M. & Martinez, M.C.** (2016) The protein kinase CK2 mediates cross-talk between auxin- and salicylic acid-signaling pathways in the regulation of PINOID transcription. *PLoS One*, **11**, e0157168.

**Baena, G., Xia, L., Waghmare, S. & Karnik, R.** (2022) SNARE SYP132 mediates divergent traffic of plasma membrane H+-ATPase AHA1 and antimicrobial PR1 during bacterial pathogenesis. *Plant Physiology*, **189**, 1639–1661.

**Barozzi, F., Papadia, P., Stefano, G., Renna, L., Brandizzi, F., Migoni, D. *et al.*** (2018) Variation in membrane trafficking linked to SNARE AtSYP51 interaction with aquaporin NIP1;1. *Frontiers in Plant Science*, **9**, 1949.

**Bassham, D.C. & Blatt, M.R.** (2008) SNAREs: cogs and coordinators in signaling and development. *Plant Physiology*, **147**, 1504–1515.

**Basu, S., Ramegowda, V., Kumar, A. & Pereira, A.** (2016) Plant adaptation to drought stress. *F1000Res*, **5**, 1554.

**Bellati, J., Champeyroux, C., Hem, S., Rofidal, V., Krouk, G., Maurel, C. *et al.*** (2016) Novel aquaporin regulatory mechanisms revealed by Interactomics. *Molecular & Cellular Proteomics*, **15**, 3473–3487.

**Besserer, A., Burnotte, E., Bienert, G.P., Chevalier, A.S., Errachid, A., Grefen, C. *et al.*** (2012) Selective regulation of maize plasma membrane aquaporin trafficking and activity by the SNARE SYP121. *Plant Cell*, **24**, 3463–3481.

**Bienert, M.D.**, **Diehn, T.A.**, **Richet, N.**, **Chaumont, F.** & **Bienert, G.P.** (2018) Heterotetramerization of plant PIP1 and PIP2 aquaporins is an evolutionary ancient feature to guide PIP1 plasma membrane localization and function. *Front Plant Sci*, **9**, 382.

**Blatt, M.R.**, **Chaumont, F.** & **Farquhar, G.** (2014) Focus on water. *Plant Physiology*, **164**, 1553–1555.

**Blatt, M.R.**, **Moore, I.**, **Batoko, H.**, **Di Sansabastiano, G.P.**, **Leyman, B.** & **Geelen, D.** (2002) Integrating control of ion channels and cell volume in guard cell signalling. *Biophysical Journal*, **82**, 3011.

**Bock, J.B.**, **Matern, H.T.**, **Peden, A.A.** & **Scheller, R.H.** (2001) A genomic perspective on membrane compartment organization. *Nature*, **409**, 839–841.

**Canessa Fortuna, A.**, **Zerbetto De Palma, G.**, **Aliperti Car, L.**, **Armentia, L.**, **Vitali, V.**, **Zeida, A.** ***et al.*** (2019) Gating in plant plasma membrane aquaporins: the involvement of leucine in the formation of a pore constriction in the closed state. *The FEBS Journal*, **286**, 3473–3487.

**Chaumont, F.**, **Moshelion, M.** & **Daniels, M.J.** (2005) Regulation of plant aquaporin activity. *Biology of the Cell*, **97**, 749–764.

**Chaumont, F.** & **Tyerman, S.D.** (2014) Aquaporins: highly regulated channels controlling plant water relations. *Plant Physiology*, **164**, 1600–1618.

**De Benedictis, M.**, **Bleve, G.**, **Faraco, M.**, **Stigliano, E.**, **Grieco, F.**, **Piro, G.** ***et al.*** (2013) AtSYP51/52 functions diverge in the post-Golgi traffic and differently affect vacuolar sorting. *Molecular Plant*, **6**, 916–930.

**Di Sansebastiano, G.P.** (2013) Defining new SNARE functions: the i-SNARE. *Frontiers in Plant Science*, **4**, 99.

**Ding, L.** & **Chaumont, F.** (2020) Are Aquaporins expressed in stomatal complexes promising targets to enhance stomatal dynamics? *Frontiers in Plant Science*, **11**, 458.

**Eisenach, C.**, **Chen, Z.H.**, **Grefen, C.** & **Blatt, M.R.** (2012) The trafficking protein SYP121 of *Arabidopsis* connects programmed stomatal closure and $K^+$ channel acivity with vegetative growth. *Plant Journal*, **69**, 241–251.

**El Kasmi, F.**, **Krause, C.**, **Hiller, U.**, **Stierhof, Y.D.**, **Mayer, U.**, **Conner, L.** ***et al.*** (2013) SNARE complexes of different composition jointly mediate membrane fusion in *Arabidopsis* cytokinesis. *Molecular Biology of the Cell*, **24**, 1593–1601.

**Enami, K.**, **Ichikawa, M.**, **Uemura, T.**, **Kutsuna, N.**, **Hasezawa, S.**, **Nakagawa, T.** ***et al.*** (2009) Differential expression control and polarized distribution of plasma membrane-resident SYP1 SNAREs in *Arabidopsis thaliana*. *Plant & Cell Physiology*, **50**, 280–289.

**Falhof, J.**, **Pedersen, J.T.**, **Fuglsang, A.T.** & **Palmgren, M.** (2016) Plasma membrane H(+)-ATPase regulation in the center of plant physiology. *Molecular Plant*, **9**, 323–337.

**Food and Agriculture Organisation of the United Nations, Rome**. (2019) *Proactive approaches to drought preparedness—Where are we now and where do we go from here?*

**Fasshauer, D.**, **Sutton, R.B.**, **Brunger, A.T.** & **Jahn, R.** (1998) Conserved structural features of the synaptic fusion complex: SNARE proteins reclassified as Q- and R-SNAREs. *Proceedings of the National Academy of Sciences of the United States of America*, **95**, 15781–15786.

**Flowers, T.J.** (2004) Improving crop salt tolerance. *Journal of Experimental Botany*, **55**, 307–319.

**Fox, A.R.**, **Scochera, F.**, **Laloux, T.**, **Filik, K.**, **Degand, H.**, **Morsomme, P.** ***et al.*** (2020) Plasma membrane aquaporins interact with the endoplasmic reticulum resident VAP27 proteins at ER-PM contact sites and endocytic structures. *The New Phytologist*, **228**, 973–988.

**Fuglsang, A.T.** & **Palmgren, M.** (2021) Proton and calcium pumping P-type ATPases and their regulation of plant responses to the environment. *Plant Physiology*, **187**, 1856–1875.

**Gigli-Bisceglia, N.** & **Testerink, C.** (2021) Fighting salt or enemies: shared perception and signaling strategies. *Current Opinion in Plant Biology*, **64**, 102120.

**Granot, D.** & **Kelly, G.** (2019) Evolution of guard-cell theories: the story of sugars. *Trends in Plant Science*, **24**, 507–518.

**Grefen, C.**, **Honsbein, A.** & **Blatt, M.R.** (2011) Ion transport, membrane traffic and cellular volume control. *Current Opinion in Plant Biology*, **14**, 332–339.

**Grefen, C.**, **Karnik, R.**, **Larson, E.**, **Lefoulon, C.**, **Wang, Y.**, **Waghmare, S.** ***et al.*** (2015) A vesicle-trafficking protein commandeers Kv channel voltage sensors for voltage-dependent secretion. *Nature Plants*, **1**, 15108.

**Grondin, A.**, **Rodrigues, O.**, **Verdoucq, L.**, **Merlot, S.**, **Leonhardt, N.** & **Maurel, C.** (2015) Aquaporins contribute to ABA-triggered stomatal closure through OST1-mediated phosphorylation. *Plant Cell*, **27**, 1945–1954.

**Groszmann, M.**, **De Rosa, A.**, **Chen, W.**, **Qiu, J.**, **McGaughey, S.A.**, **Byrt, C.S.** ***et al.*** (2023) A high-throughput yeast approach to characterize aquaporin permeabilities: profiling the *Arabidopsis* PIP aquaporin sub-family. *Frontiers in Plant Science*, **14**, 1078220.

**Gupta, A.**, **Rico-Medina, A.** & **Cano-Delgado, A.I.** (2020) The physiology of plant responses to drought. *Science*, **368**, 266–269.

**Hachez, C.**, **Besserer, A.**, **Chevalier, A.S.** & **Chaumont, F.** (2013) Insights into plant plasma membrane aquaporin trafficking. *Trends in Plant Science*, **18**, 344–352.

**Hachez, C.**, **Laloux, T.**, **Reinhardt, H.**, **Cavez, D.**, **Degand, H.**, **Grefen, C.** ***et al.*** (2014) *Arabidopsis* SNAREs SYP61 and SYP121 coordinate the trafficking of plasma membrane aquaporin PIP2;7 to modulate the cell membrane water permeability. *Plant Cell*, **26**, 3132–3147.

**Hager, A.** (2003) Role of the plasma membrane H+-ATPase in auxin-induced elongation growth: historical and new aspects. *Journal of Plant Research*, **116**, 483–505.

**Hager, A.**, **Debus, G.**, **Edel, H.G.**, **Stransky, H.** & **Serrano, R.** (1991) Auxin induces exocytosis and the rapid synthesis of a high-turnover pool of plasma-membrane H(+)-ATPase. *Planta*, **185**, 527–537.

**Hager, A.**, **Frenzel, R.** & **Laible, D.** (1980) ATP-dependent proton transport into vesicles of microsomal membranes of Zea mays coleoptiles. *Zeitschrift fur Naturforschung. Section C: Biosciences*, **35**, 783–793.

**Hager, A.** & **Moser, I.** (1985) Acetic acid esters and permeable weak acids induce active proton extrusion and extension growth of coleoptile segments by lowering the cytoplasmic pH. *Planta*, **163**, 391–400.

**Haruta, M.**, **Gray, W.M.** & **Sussman, M.R.** (2015) Regulation of the plasma membrane proton pump (H(+)-ATPase) by phosphorylation. *Current Opinion in Plant Biology*, **28**, 68–75.

**Hetherington, A.M.** & **Woodward, F.I.** (2003) The role of stomata in sensing and driving environmental change. *Nature*, **424**, 901–908.

**Honsbein, A.**, **Blatt, M.R.** & **Grefen, C.** (2011) A molecular framework for coupling cellular volume and osmotic solute transport control. *Journal of Experimental Botany*, **62**, 2363–2370.

**Honsbein, A.**, **Sokolovski, S.**, **Grefen, C.**, **Campanoni, P.**, **Pratelli, R.**, **Paneque, M.** ***et al.*** (2009) A tripartite SNARE-$K^+$ channel complex mediates in channel-dependent $K^+$ nutrition in *Arabidopsis*. *Plant Cell*, **21**, 2859–2877.

**Huang, C.J.**, **Wang, X.H.**, **Huang, J.Y.**, **Zhang, C.G.** & **Chen, Y.L.** (2020) Phosphorylation of plasma membrane aquaporin PIP2;1 in C-terminal affects light-induced stomatal opening in Arabidopsis. *Plant Signaling & Behavior*, **15**, 1795394.

**Ichikawa, M.**, **Hirano, T.**, **Enami, K.**, **Fuselier, T.**, **Kato, N.**, **Kwon, C.** ***et al.*** (2014) Syntaxin of plant proteins SYP123 and SYP132 mediate root hair tip growth in *Arabidopsis thaliana*. *Plant & Cell Physiology*, **55**, 790–800.

**Israel, D.**, **Khan, S.**, **Warren, C.R.**, **Zwiazek, J.J.** & **Robson, T.M.** (2021) The contribution of PIP2-type aquaporins to photosynthetic response to increased vapour pressure deficit. *Journal of Experimental Botany*, **72**, 5066–5078.

**Jang, J.Y.**, **Kim, D.G.**, **Kim, Y.O.**, **Kim, J.S.** & **Kang, H.** (2004) An expression analysis of a gene family encoding plasma membrane aquaporins in response to abiotic stresses in *Arabidopsis thaliana*. *Plant Molecular Biology*, **54**, 713–725.

**Janicka-Russak, M.**, **Kabała, K.**, **Wdowikowska, A.** & **Kłobus, G.** (2013) Modification of plasma membrane proton pumps in cucumber roots as an adaptation mechanism to salt stress. *Journal of Plant Physiology*, **170**, 915–922.

**Jezek, M.** & **Blatt, M.R.** (2017) The membrane transport system of the guard cell and its integration for stomatal dynamics. *Plant Physiology*, **174**, 487–519.

**Jezek, M.**, **Hills, A.**, **Blatt, M.R.** & **Lew, V.L.** (2019) A constraint-relaxation-recovery mechanism for stomatal dynamics. *Plant, Cell & Environment*, **42**, 2399–2410.

**Jezek, M.**, **Silva-Alvim, F.A.L.**, **Hills, A.**, **Donald, N.**, **Ishka, M.R.**, **Shadbolt, J.** ***et al.*** (2021) Guard cell endomembrane Ca(2+)-ATPases underpin a 'carbon memory' of photosynthetic assimilation that impacts on water-use efficiency. *Nature Plants*, **7**, 1301–1313.

**Jozefkowicz, C.**, **Sigaut, L.**, **Scochera, F.**, **Soto, G.**, **Ayub, N.**, **Pietrasanta, L.I.** ***et al.*** (2016) PIP water transport and its pH dependence are regulated by tetramer stoichiometry. *Biophys J*, **110**, 1312–1321.

**Jürgens, G.** (2004) Membrane trafficking in plants. *Annual Review of Cell and Developmental Biology*, **20**, 481–504.

**Kalde, M.**, **Nuhse, T.S.**, **Findlay, K.** & **Peck, S.C.** (2007) The syntaxin SYP132 contributes to plant resistance against bacteria and secretion of pathogenesis-related protein 1. *Proceedings of the National Academy of Sciences of the United States of America*, **104**, 11850–11855.

**Karimi, S.M.**, **Freund, M.**, **Wager, B.M.**, **Knoblauch, M.**, **Fromm, J.**, **M Mueller, H. *et al.*** (2021) Under salt stress guard cells rewire ion transport and abscisic acid signaling. *New Phytologist*, **231**, 1040–1055.

**Karnik, R.**, **Waghmare, S.**, **Zhang, B.**, **Larson, E.**, **Lefoulon, C.**, **Gonzalez, W. *et al.*** (2017) Commandeering channel voltage sensors for secretion, cell turgor, and volume control. *Trends in Plant Science*, **22**, 81–95.

**Kaundal, A.**, **Ramu, V.S.**, **Oh, S.**, **Lee, S.**, **Pant, B.**, **Lee, H.K. *et al.*** (2017) GENERAL CONTROL NONREPRESSIBLE4 degrades 14-3-3 and the RIN4 complex to regulate stomatal aperture with implications on nonhost disease resistance and drought tolerance. *Plant Cell*, **29**, 2233–2248.

**Kim, H.S.**, **Park, W.**, **Lee, H.S.**, **Shin, J.H.** & **Ahn, S.J.** (2020) Subcellular journey of rare cold inducible 2 protein in plant under stressful condition. *Front Plant Sci*, **11**, 610251.

**Kim, Y.-O.**, **Kim, H.-S.**, **Lim, H.-G.**, **Jang, H.-Y.**, **Kim, E.** & **Ahn, S.-J.** (2022) Functional characterization of salt-stress induced Rare cold inducible gene from Camelina sativa (CsRCI2D). *Journal Of Plant Biology*, **65**, 279–289.

**Kim, Y.-O.**, **Lim, H.-G.**, **Kim, H.-S.** & **Ahn, S.-J.** (2020) Overexpression of CsRCI2H enhances salt tolerance in *Camelina sativa* (L.). *Plant Biotechnol Rep*, **14**, 439–449.

**Klejchova, M.**, **Silva-Alvim, F.A.L.**, **Blatt, M.R.** & **Alvim, J.C.** (2021) Membrane voltage as a dynamic platform for spatiotemporal signaling, physiological, and developmental regulation. *Plant Physiology*, **185**, 1523–1541.

**Kwon, C.**, **Lee, J.H.** & **Yun, H.S.** (2020) SNAREs in plant biotic and abiotic stress responses. *Molecules and Cells*, **43**, 501–508.

**Laloux, T.**, **Matyjaszczyk, I.**, **Beaudelot, S.**, **Hachez, C.** & **Chaumont, F.** (2020) Interaction between the SNARE SYP121 and the plasma membrane aquaporin PIP2;7 involves different protein domains. *Frontiers in Plant Science*, **11**, 631643.

**Lawson, T.** & **Blatt, M.R.** (2014) Stomatal size, speed, and responsiveness impact on photosynthesis and water use efficiency. *Plant Physiology*, **164**, 1556–1570.

**Li, X.**, **Wang, X.**, **Yang, Y.**, **Li, R.**, **He, Q.**, **Fang, X. *et al.*** (2011) Single-molecule analysis of PIP2;1 dynamics and partitioning reveals multiple modes of Arabidopsis plasma membrane aquaporin regulation. *Plant Cell*, **23**, 3780–3797.

**Lin, R.C.** & **Scheller, R.H.** (2000) Mechanisms of synaptic vesicle exocytosis. *Annual Review of Cell and Developmental Biology*, **16**, 19–49.

**Liu, J.**, **Elmore, J.M.**, **Fuglsang, A.T.**, **Palmgren, M.G.**, **Staskawicz, B.J.** & **Coaker, G.** (2009) RIN4 functions with plasma membrane H+-ATPases to regulate stomatal apertures during pathogen attack. *PLoS Biology*, **7**, e1000139.

**Liu, X.**, **Liu, W.**, **Tang, Q.**, **Liu, B.**, **Wada, Y.** & **Yang, H.** (2022) Global agricultural water scarcity assessment incorporating blue and green water availability under future climate change. *Earth's Future*, **10**, e2021EF002567.

**Liu, Z.**, **Hou, S.**, **Rodrigues, O.**, **Wang, P.**, **Luo, D.**, **Munemasa, S. *et al.*** (2022) Phytocytokine signalling reopens stomata in plant immunity and water loss. *Nature*, **605**, 332–339.

**Livak, K.J.** & **Schmittgen, T.D.** (2001) Analysis of relative gene expression data using real-time quantitative PCR and the 2(-Delta Delta C(T)) method. *Methods*, **25**, 402–408.

**Luu, D.T.** & **Maurel, C.** (2013) Aquaporin trafficking in plant cells: an emerging membrane-protein model. *Traffic*, **14**, 629–635.

**Ma, X.**, **Su, Z.** & **Ma, H.** (2020) Molecular genetic analyses of abiotic stress responses during plant reproductive development. *Journal of Experimental Botany*, **71**, 2870–2885.

**Maurel, C.**, **Boursiac, Y.**, **Luu, D.T.**, **Santoni, V.**, **Shahzad, Z.** & **Verdoucq, L.** (2015) Aquaporins in plants. *Physiological Reviews*, **95**, 1321–1358.

**Maurel, C.** & **Chrispeels, M.J.** (2001) Aquaporins. A molecular entry into plant water relations. *Plant Physiology*, **125**, 135–138.

**Maurel, C.**, **Verdoucq, L.** & **Rodrigues, O.** (2016) Aquaporins and plant transpiration. *Plant, Cell & Environment*, **39**, 2580–2587.

**Meckel, T.**, **Gall, L.**, **Semrau, S.**, **Homann, U.** & **Thiel, G.** (2007) Guard cells elongate: relationship of volume and surface area during stomatal movement. *Biophysical Journal*, **92**, 1072–1080.

**Melotto, M.**, **Zhang, L.**, **Oblessuc, P.R.** & **He, S.Y.** (2017) Stomatal defense a decade later. *Plant Physiology*, **174**, 561–571.

**Michelet, B.** & **Boutry, M.** (1995) The plasma membrane H+-ATPase (a highly regulated enzyme with multiple physiological functions). *Plant Physiology*, **108**, 1–6.

**Munns, R.**, **James, R.A.** & **Lauchli, A.** (2006) Approaches to increasing the salt tolerance of wheat and other cereals. *Journal of Experimental Botany*, **57**, 1025–1043.

**Munns, R.** & **Tester, M.** (2008) Mechanisms of salinity tolerance. *Annual Review of Plant Biology*, **59**, 651–681.

**Palmgren, M.** & **Morsomme, P.** (2019) The plasma membrane H+-ATPase, a simple polypeptide with a long history. *Yeast*, **36**, 201–210.

**Pandey, P.**, **Ramegowda, V.** & **Senthil-Kumar, M.** (2015) Shared and unique responses of plants to multiple individual stresses and stress combinations: physiological and molecular mechanisms. *Frontiers in Plant Science*, **6**, 723.

**Paudel, I.**, **Cohen, S.**, **Shlizerman, L.**, **Jaiswal, A.K.**, **Shaviv, A.** & **Sadka, A.** (2017) Reductions in root hydraulic conductivity in response to clay soil and treated waste water are related to PIPs down-regulation in citrus. *Scientific Reports*, **7**, 15429.

**Perez-Riverol, Y.**, **Bai, J.**, **Bandla, C.**, **Garcia-Seisdedos, D.**, **Hewapathirana, S.**, **Kamatchinathan, S. *et al.*** (2022) The PRIDE database resources in 2022: a hub for mass spectrometry-based proteomics evidences. *Nucleic Acids Research*, **50**, D543–D552.

**Postaire, O.**, **Tournaire-Roux, C.**, **Grondin, A.**, **Boursiac, Y.**, **Morillon, R.**, **Schäffner, A.R. *et al.*** (2010) A PIP1 aquaporin contributes to hydrostatic pressure-induced water transport in both the root and rosette of *Arabidopsis*. *Plant Physiology*, **152**, 1418–1430.

**Prado, K.**, **Boursiac, Y.**, **Tournaire-Roux, C.**, **Monneuse, J.-M.**, **Postaire, O.**, **Da Ines, O. *et al.*** (2013) Regulation of *Arabidopsis* leaf hydraulics involves light-dependent phosphorylation of Aquaporins in veins. *Plant Cell*, **25**, 1029–1039.

**Pratelli, R.**, **Sutter, J.U.** & **Blatt, M.R.** (2004) A new catch in the SNARE. *Trends in Plant Science*, **9**, 187–195.

**Rehman, R.U.**, **Stigliano, E.**, **Lycett, G.W.**, **Sticher, L.**, **Sbano, F.**, **Faraco, M. *et al.*** (2008) Tomato Rab11a characterization evidenced a difference between SYP121-dependent and SYP122-dependent exocytosis. *Plant and Cell Physiology*, **49**, 751–766.

**Rodrigues, O.**, **Reshetnyak, G.**, **Grondin, A.**, **Saijo, Y.**, **Leonhardt, N.**, **Maurel, C. *et al.*** (2017) Aquaporins facilitate hydrogen peroxide entry into guard cells to mediate ABA- and pathogen-triggered stomatal closure. *Proceedings of the National Academy of Sciences of the United States of America*, **114**, 9200–9205.

**Rodriguez-Furlan, C.**, **Minina, E.A.** & **Hicks, G.R.** (2019) Remove, recycle, degrade: regulating plasma membrane protein accumulation. *The Plant Cell*, **31**, 2833–2854.

**Sade, N.**, **Galkin, E.** & **Moshelion, M.** (2015) Measuring *Arabidopsis*, tomato and barley leaf relative water content (RWC). *Bio-Protocol*, **5**, e1451.

**Sadura, I.**, **Libik-Konieczny, M.**, **Jurczyk, B.**, **Gruszka, D.** & **Janeczko, A.** (2020) Plasma membrane ATPase and the aquaporin HvPIP1 in barley brassinosteroid mutants acclimated to high and low temperature. *Journal of Plant Physiology*, **244**, 153090.

**Saijo, Y.** & **Loo, E.P.** (2020) Plant immunity in signal integration between biotic and abiotic stress responses. *The New Phytologist*, **225**, 87–104.

**Shibasaka, M.**, **Horie, T.** & **Katsuhara, M.** (2021) Mechanisms activating latent functions of PIP aquaporin water channels via the interaction between PIP1 and PIP2 proteins. *Plant Cell Physiol*, **62**, 92–99.

**Sondergaard, T.E.**, **Schulz, A.** & **Palmgren, M.G.** (2004) Energization of transport processes in plants. Roles of the plasma membrane H+-ATPase. *Plant Physiology*, **136**, 2475–2482.

**Sutter, J.U.**, **Sieben, C.**, **Hartel, A.**, **Eisenach, C.**, **Thiel, G.** & **Blatt, M.R.** (2007) Abscisic acid triggers the endocytosis of the *Arabidopsis* KAT1 K+ channel and its recycling to the plasma membrane. *Current Biology*, **17**, 1396–1402.

**Sze, H.**, **Li, X.H.** & **Palmgren, M.G.** (1999) Energization of plant cell membranes by $H^+$ –pumping ATPases: regulation and biosynthesis. *Plant Cell*, **11**, 677–689.

**Ueda, M.**, **Tsutsumi, N.** & **Fujimoto, M.** (2016) Salt stress induces internalization of plasma membrane aquaporin into the vacuole in *Arabidopsis thaliana*. *Biochemical and Biophysical Research Communications*, **474**, 742–746.

**Vavasseur, A.** & **Raghavendra, A.S.** (2005) Guard cell metabolism and CO2 sensing. *New Phytologist*, **165**, 665–682.

**Verdoucq, L.**, **Grondin, A.** & **Maurel, C.** (2008) Structure-function analysis of plant aquaporin AtPIP2;1 gating by divalent cations and protons. *The Biochemical Journal*, **415**, 409–416.

**Verdoucq, L.**, **Rodrigues, O.**, **Martiniere, A.**, **Luu, D.T.** & **Maurel, C.** (2014) Plant aquaporins on the move: reversible phosphorylation, lateral motion and cycling. *Current Opinion in Plant Biology*, **22**, 101–107.

**Verslues, P.E.**, **Agarwal, M.**, **Katiyar-Agarwal, S.**, **Zhu, J.** & **Zhu, J.K.** (2006) Methods and concepts in quantifying resistance to drought, salt and freezing, abiotic stresses that affect plant water status. *The Plant Journal*, **45**, 523–539.

**Vialet-Chabrand, S.R.M.**, **Matthews, J.S.A.**, **McAusland, L.**, **Blatt, M.R.**, **Griffiths, H.** & **Lawson, T.** (2017) Temporal dynamics of stomatal behavior: modeling and implications for photosynthesis and water use. *Plant Physiology*, **174**, 603–613.

**Vilakazi, C.S.**, **Dubery, I.A.** & **Piater, L.A.** (2017) Identification of lipopolysaccharide-interacting plasma membrane-type proteins in *Arabidopsis thaliana*. *Plant Physiology and Biochemistry*, **111**, 155–165.

**Virk, N.**, **Li, D.**, **Tian, L.**, **Huang, L.**, **Hong, Y.**, **Li, X.** ***et al.*** (2015) *Arabidopsis* Raf-like mitogen-activated protein kinase kinase kinase gene Raf43 is required for tolerance to multiple abiotic stresses. *PLoS One*, **10**, e0133975.

**Waghmare, S.**, **Lileikyte, E.**, **Karnik, R.**, **Goodman, J.K.**, **Blatt, M.R.** & **Jones, A.M.E.** (2018) SNAREs SYP121 and SYP122 mediate the secretion of distinct cargo subsets. *Plant Physiology*, **178**, 1679–1688.

**Wang, Y.**, **Blatt, M.R.** & **Chen, Z.-H.** (2018) Ion transport at the plant plasma membrane. In *eLS*. Chichester: John Wiley & Sons, Ltd. https://doi.org/10.1002/9780470015902.a0001307.pub3

**Wehner, M.F.A.A.J.R.**, **Knutson, T.**, **Kunkel, K.E.** & **LeGrande, A.N.** (2017) Droughts, floods, and wildfires. In: Wuebbles, D.J.A.F.D.W., Hibbard, K.A., Dokken, D.J., Stewart, B.C. & Maycock, T.K. (Eds.) *Climate Science Special Report: Fourth National Climate Assessment, Volume I*. Washington, D.C.: U.S. Global Change Research Program, pp. 231–256.

**Wisniewski, J.R.**, **Zougman, A.**, **Nagaraj, N.** & **Mann, M.** (2009) Universal sample preparation method for proteome analysis. *Nature Methods*, **6**, 359–362.

**Wudick, M.M.**, **Li, X.**, **Valentini, V.**, **Geldner, N.**, **Chory, J.**, **Lin, J.** ***et al.*** (2015) Subcellular redistribution of root aquaporins induced by hydrogen peroxide. *Molecular Plant*, **8**, 1103–1114.

**Xia, L.**, **Mar Marques-Bueno, M.**, **Bruce, C.G.** & **Karnik, R.** (2019) Unusual roles of secretory SNARE SYP132 in plasma membrane H(+)-ATPase traffic and vegetative plant growth. *Plant Physiology*, **180**, 837–858.

**Xia, L.**, **Mar Marques-Bueno, M.** & **Karnik, R.** (2020) Trafficking SNARE SYP132 partakes in auxin-associated root growth. *Plant Physiology*, **182**, 1836–1840.

**Xue, Y.**, **Yang, Y.**, **Yang, Z.**, **Wang, X.** & **Guo, Y.** (2018) VAMP711 is required for abscisic acid-mediated inhibition of plasma membrane H(+)-ATPase activity. *Plant Physiology*, **178**, 1332–1343.

**Yamauchi, S.**, **Takemiya, A.**, **Sakamoto, T.**, **Kurata, T.**, **Tsutsumi, T.**, **Kinoshita, T.** ***et al.*** (2016) The plasma membrane $H^+$-ATPase AHA1 plays a major role in stomatal opening in response to blue light. *Plant Physiology*, **171**, 2731–2743.

**Yang, B.** (2017) Advances in experimental medicine and biology 969 aquaporins. *Springer Science+ Business Media BV*, **10**, 978–994.

**Zelazny, E.**, **Borst, J.W.**, **Muylaert, M.**, **Batoko, H.**, **Hemminga, M.A.** & **Chaumont, F.** (2007) FRET imaging in living maize cells reveals that plasma membrane aquaporins interact to regulate their subcellular localization. *Proc Natl Acad Sci USA*, **104**, 12359–12364.

**Zhang, B.**, **Karnik, R.**, **Donald, N.** & **Blatt, M.R.** (2018) A GPI signal peptide-anchored split-ubiquitin (GPS) system for detecting Soluble bait protein interactions at the membrane. *Plant Physiology*, **178**, 13–17.

**Zhang, B.**, **Karnik, R.**, **Wang, Y.**, **Wallmeroth, N.**, **Blatt, M.R.** & **Grefen, C.** (2015) The *Arabidopsis* R-SNARE VAMP721 interacts with KAT1 and KC1 $K^+$ channels to moderate $K^+$ current at the plasma membrane. *Plant Cell*, **27**, 1697–1717.

**Zhang, B.**, **Xia, L.**, **Zhang, Y.**, **Wang, H.** & **Karnik, R.** (2021) Tri-SUS: a yeast split-ubiquitin assay to examine protein interactions governed by a third binding partner. *Plant Physiology*, **185**, 285–289.

**Zhang, H.**, **Zhao, Y.** & **Zhu, J.-K.** (2020) Thriving under stress: how plants balance growth and the stress response. *Developmental Cell*, **55**, 529–543.

**Zhang, H.**, **Zhu, J.**, **Gong, Z.** & **Zhu, J.-K.** (2022) Abiotic stress responses in plants. *Nature Reviews Genetics*, **23**, 104–119.

**Zhang, L.**, **Chen, L.** & **Dong, H.** (2019) Plant aquaporins in infection by and immunity against pathogens—a critical review. *Frontiers in Plant Science*, **10**, 632.

**Zhang, M.**, **Shi, H.**, **Li, N.**, **Wei, N.**, **Tian, Y.**, **Peng, J.** ***et al.*** (2022) Aquaporin OsPIP2;2 links the $H_2O_2$ signal and a membrane-anchored transcription factor to promote plant defense. *Plant Physiology*, **188**, 2325–2341.

**Zonia, L.** & **Munnik, T.** (2007) Life under pressure: hydrostatic pressure in cell growth and function. *Trends in Plant Science*, **12**, 90–97.